Catena 207 (2021) 105698

Contents lists available at ScienceDirect

Catena

journal homepage: www.elsevier.com/locate/catena

Have land use and land cover change affected soil thickness and weathering degree in a subtropical region in Southern Brazil? Insights from applied mid-infrared spectroscopy

Liesa Brosens [a,b,*], Jérémy Robinet [a], Ignace Pelckmans [c], Yolanda Ameijeiras-Mariño [d], Gerard Govers [a], Sophie Opfergelt [d], Jean P.G. Minella [e], Jan Vanderborght [f,g]

[a] Division of Geography and Tourism, Department of Earth and Environmental Sciences, KU Leuven, Leuven, Belgium
[b] Research Foundation Flanders (FWO), Egmontstraat 5, 1000 Brussels, Belgium
[c] Department of Biology, University of Antwerp, Antwerp, Belgium
[d] Earth and Life Institute, Environmental Sciences, Université catholique de Louvain, Belgium
[e] Department of Soil, Universidade Federal de Santa Maria, Rio Grande do Sul, Brazil
[f] Institute of Bio- and Geosciences, IBG-3: Agrosphere, Forschungszentrum Jülich GmbH, Jülich, Germany
[g] Division of Soil and Water Management, Department of Earth and Environmental Sciences, KU Leuven, Leuven, Belgium

ARTICLE INFO

Keywords:
Critical zone
(sub-) tropical environment
Soil degradation
Chemical weathering indices

ABSTRACT

Land use and land cover changes (LUCC) can drastically alter various components of the critical zone, including soil thickness and soil chemical weathering processes. Often these studies, however, tend to focus on extreme cases, not representing what actually happens on average at larger, regional scales. Here, we evaluate the impact of LUCC on soil thickness and soil weathering degree at the regional scale, where we use soil spectroscopy to derive weathering indices. In a subtropical region in Southern Brazil, we collected calibration/validation soil samples (n = 49) from 4 different locations for which we measured the mid-infrared (MIR) spectral reflectance and 3 soil chemical weathering indices: chemical index of alteration (CIA), the total reserve in bases (TRB), and the iron ratio (Fe_d/Fe_t). We used partial least square regressions on this calibration/validation dataset to relate the MIR spectra of the soil samples to these weathering indices, resulting in good calibration relationships with R^2 values of 0.97, 0.91 and 0.84 for CIA, TRB and Fe_d/Fe_t, respectively. Applying these relations to MIR spectra of regionally collected soil samples allowed us to calculate soil weathering degrees for a large number of soil samples (n = 229), without requiring costly and time-consuming chemical analyses. We collected these soil samples at 100 mid-slope positions: 50 under forest and 50 under agricultural land use. Land use explained only a minor part of the variation in soil thickness and weathering degree. Thus, while local water and tillage erosion rates might be considerable after deforestation, this has not led to significant reductions in average soil thickness and has not affected soil weathering degree. Slope gradient is the main factor influencing the spatial variability in soil thickness and weathering degree on mid-slope sections in our study area. Human activities over the last century did not fundamentally alter these patterns.

1. Introduction

The critical zone (CZ) is the outer layer of the Earth's surface, extending from the upper limit of the vegetation down to the groundwater. The CZ provides nutrients and energy for terrestrial ecosystems through a complex interplay of biogeochemical processes (Brantley et al., 2007). Increasing demand for agricultural land, due to the growing world population and changing food patterns, has drastically increased deforestation and land use and land cover change (LUCC) (Foley, 2011; Godfray et al., 2010; Lal, 2001). These changes have been documented to strongly impact different components of the critical zone, leading to reduced soil organic carbon content (e.g. Don et al., 2011; Guo and Gifford, 2002; Veldkamp, 1994) and significant alterations in soil physical properties (e.g. Alegre et al., 1986; Lemenih et al., 2005; Haghighi et al., 2010; Trabaquini et al., 2015). Not only physical soil properties, but also soil chemistry and weathering are influenced by

* Corresponding author at: Division of Geography and Tourism, Department of Earth and Environmental Sciences, KU Leuven, Leuven, Belgium.
E-mail address: liesa.brosens@kuleuven.be (L. Brosens).

https://doi.org/10.1016/j.catena.2021.105698
Received 16 March 2021; Received in revised form 16 August 2021; Accepted 22 August 2021
Available online 8 September 2021

forest conversion to cropland, which can decrease the acidity of soils (Ameijeiras-Mariño et al., 2018; Lucas, 2001), especially due to the disturbance of the acidic upper layer of the forested soil profiles (Lundström, 1994), and the application of fertilizers and lime (Cornu et al., 2007; van Breemen et al., 1983). Such external inputs have been linked to changes in soil acidity (Cornu et al., 2007; Goulding, 2016; van Breemen et al., 1983) and clay mineralogy (Bortoluzzi et al., 2012; Caner et al., 2014) and could therefore influence soil formation and weathering dynamics.

In addition, agricultural practices often lead to rapid land degradation due to an increase in soil erosion (Lal, 2001), either because of a change in hydrological pathways towards increased surface runoff (de Moraes et al., 2006; Robinet et al., 2018a; Salemi et al., 2013), or because of tillage erosion (Govers et al., 1996, 1994; Van Oost et al., 2006). Increased soil erosion rates have also been linked to a reduction in soil thickness (Bakker et al., 2004). The latter can be expected to also affect soil chemical properties such as the soil weathering degree, which may, in turn, affect soil functioning, as it controls nutrient availability and nutrient retention. Thus, anthropogenic activities can strongly affect soil development and functioning. This is particularly the case in (sub-) tropical environments, where LUCC has been taking place mainly in the last decades and where weathering processes are intense due to a combination of high temperatures and high precipitation (Lambin et al., 2003; Lepers et al., 2005; McDowell and Asbury, 1994; White et al., 1998).

Studies focusing on the effect of land use change and anthropogenic activities on soils have hitherto mostly used pairwise comparisons, whereby plots subject to more or less intense human disturbance are compared with pristine sites. This might pose a risk of bias as we often tend to measure differences where we expect them to be significant. Auerswald et al. (2009) and Cerdan et al. (2006) showed that the average slope of erosion plots in Germany and Europe is much higher than the average slope of arable land, resulting in a strong overestimation of soil erosion when erosion rates measured on plots are directly extrapolated to all arable land. Furthermore, there is the risk that non-significant results are not reported in the literature, a bias that has been found in many other fields e.g. ecology (Lortie et al., 2007), social sciences (Franco et al., 2014) and medicine (Dwan et al., 2013). It is likely that underreporting of non-significant results also occurs in soil science, which might seriously threat the validity of *meta*-analyses (Kicinski, 2014). Another issue is that experimental plots might not fully reflect the reality at the regional- or landscape scale. This is, for example, illustrated by the dampening effect of field borders on erosion and deposition, which becomes only apparent at the landscape scale (Chartin et al., 2013; Houben, 2008). The importance of long-term measurements at the landscape scale was also highlighted by Fiener et al., (2019), who showed that these are crucial in order to capture important long-term spatio-temporal variations. These issues impose the need to address anthropogenic impacts on soil degradation not only at the point- or plot scale, but also at the regional- or landscape scale.

Many studies suggest that soil degradation, and soil erosion in particular, is nowadays more important in tropical and subtropical settings rather than in temperate regions (e.g. Labrière et al., 2015; Panagos et al., 2017). Nevertheless, studies assessing the impact of LUCC on soil truncation by erosion and/or soil weathering in tropical and subtropical settings at a regional scale are hitherto lacking. There is therefore a risk that there is an over-reliance on point or plot data to assess the magnitude of the effects of LUCC on soil properties and soil functioning in these landscapes, resulting in an imperfect understanding.

Here, we use a pseudo-randomly sampled regional dataset to assess i) the applicability of soil spectroscopy to measure soil weathering indices, ii) the impact of LUCC on soil thickness, and iii) the impact of LUCC on soil weathering degree. We do so by sampling the mid-slope position of 50 forest and 50 agricultural hillslopes for a variety of slope gradients in a subtropical soil-covered region in Southern Brazil. Soil thickness was measured at each location and the weathering degree was determined by considering three weathering indices: the chemical index of alteration (CIA), the total reserve in bases (TRB) and the iron ratio (Fe_d/Fe_t). Based on a catena-scale calibration/validation dataset, collected within our study area, we first develop calibration relationships between these weathering indices and the soil's spectral characteristics measured in the MIR-region. Next, we apply the obtained calibrations to our regionally collected soil samples and investigate to what extent soil thickness and weathering degree are affected by environmental controls such as topography and land use.

2. Material and methods

2.1. Study area

Our study area of ca. 250 km^2 is located at the southern edge of the Paraná Basin plateau in the "Serra Gerral" region in Rio Grande do Sul, which was formed during the lower Cretaceous (ca. 127–137 Myr ago, Renne et al., 1992; Turner et al., 1994; Vieira et al., 2015 - Fig. 1). The lithology is mainly composed of basalt with rhyodacite often found on top (Bellieni et al., 1986; Ernesto et al., 1990; Renne et al., 1992). At the altitude range of our study area (370–790 m), the principal parent material is rhyodacite (Bellieni et al., 1986) with a sanidine and quartz dominated mineralogy (Ameijeiras-Mariño et al., 2018). Steep slopes (generally $> 20^\circ$), due to the incision of rivers into the plateau, and gentle slopes (generally $< 10^\circ$), located on the remnants of the incised plateau, characterize the topography (Fig. 1). The main soil types in our study area are deep Acrisols on gentler slopes and shallow Leptosols on steeper slopes, but some profiles are classified as Cambisols (IUSS Working Group WRB, 2015; IBGE, 2003). A thick saprolite layer is often found at the interface between the soil and the bedrock. The climate in the region corresponds to a subtropical climate without a dry season and with a temperate summer (Cfb according to the Köppen Classification, Alvares et al., 2014). Precipitation is well distributed throughout the year with annual rainfall amounts around 1900 mm and average temperatures ranging from 12 °C in July to 22 °C in January (Robinet et al., 2018b, 2018a).

The natural vegetation in our study area consists of mixed Ombrophilous forest (Araucaria forest), an ecoregion part of the Atlantic Forest (Morellato and Haddad, 2000). Since the beginning of the 20th century, colonization of the area has led to an intensive conversion of forest to agricultural land use (Lopes, 2006, Fig. 1b). As a result, up to around 90% of the original forest cover has been converted to agricultural land (Ribeiro et al., 2009). The main crops in the region are tobacco (*Nicotina tabacum*) and erva-mate (*Ilex paraguariensis*) on the steeper slopes, and soybean (*Glycine* max) on the gentler slopes. Some areas were recently reforested with Eucalyptus (*Eucalyptus* spp.) and pasture can be found at higher elevations on the plateau. An intensive cultivation with poor traditional agricultural practices has led to soil degradation (Le Gall et al., 2017; Minella et al., 2009), mainly linked to an increase in surface runoff (Minella et al., 2009; Robinet et al., 2018a).

Within this broader study area of ca. 250 km^2 two datasets were used: i) a calibration/validation dataset consisting of 49 soil samples collected on 4 catena located in a forested and agricultural catchment (grey starts Fig. 1.a) which was published in Vanacker et al. (2019), and ii) a newly collected regional dataset consisting of 100 sampled hillslopes (50 under forest and 50 under agriculture, white and black dots in Fig. 1), resulting in 229 collected soil samples. The samples of the calibration/validation dataset are used to establish a relationship between measured weathering indices and scanned soil spectra, which is then applied to the spectra of the regionally collected database. The impact of LUCC on weathering degree that was currently only studied at the catena-scale could in this way be assessed at a wider regional scale. Both datasets are described in detail in the sections below and are summarized in Fig. A1.

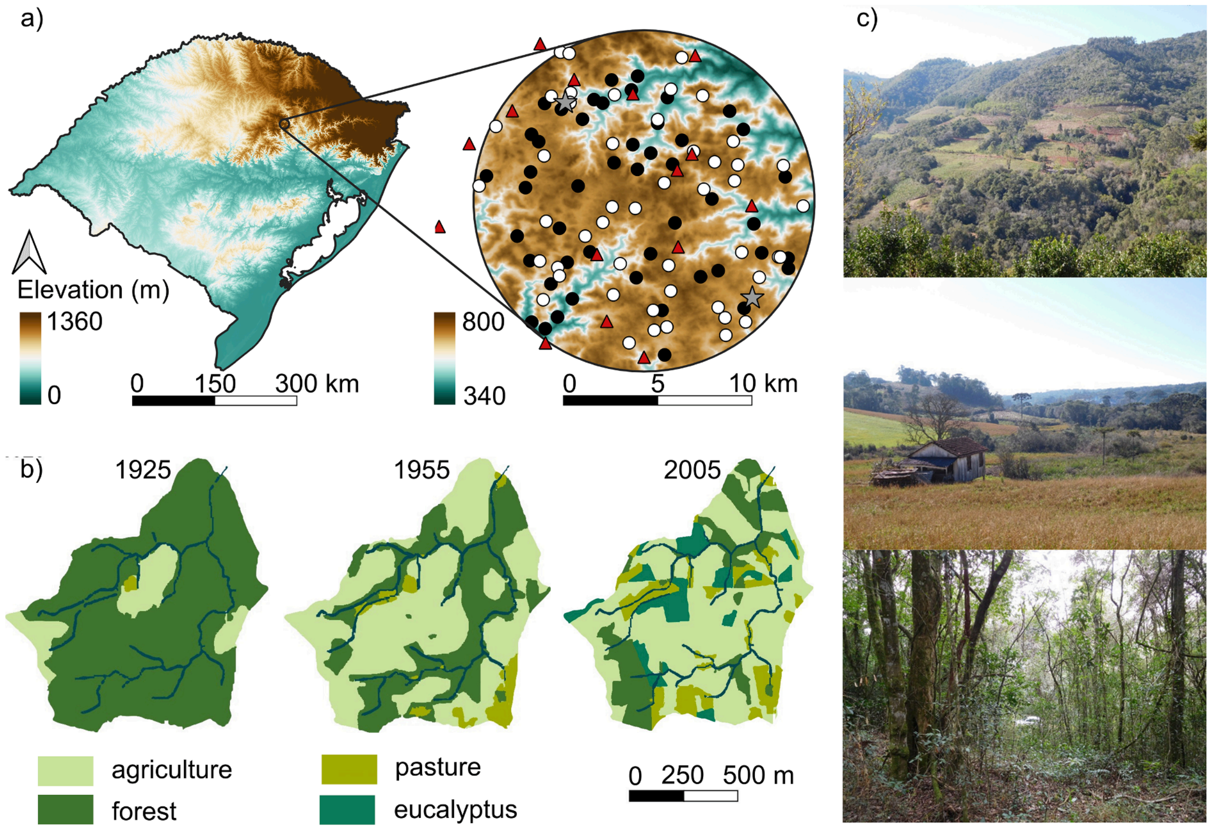

Fig. 1. a) Location of the study area (ca. 250 km^2) within the state of Rio Grande do Sul (Brazil) and location of the forest (white circles) and agricultural (black circles) sites selected for regional soil sampling. The two catchments where calibration/validation sites are located (grey stars – forest at SE, agriculture at NW) and the sites of bedrock sampling (red triangles) are also indicated. Elevations are in meters a.s.l. b) Land use change in the Arvorezinha catchment from 1925 to 2005, located within the study area. Maps are adapted from Lopes (2006). c) pictures illustrating the typical land use and landscape of the study area, consisting of a mosaic of native forest, agriculture and eucalypt plantations on steeply incised hillslopes. Pictures taken in July 2016 by L. Brosens. (For interpretation of the references to color in this figure legend, the reader is referred to the web version of this article.)

2.2. Calibration/validation dataset: Chemical analyses and weathering indices

The calibration/validation dataset consists of samples that were collected in two watersheds with contrasting land uses (forest (FO) vs. agriculture (AR), grey stars Fig. 1a) that were intensively studied within the framework of ‘The Soil system under Global Change (SOGLO)’ project (Ameijeiras-Mariño et al., 2018; Robinet et al., 2018a, 2018b; Schoonejans et al., 2017; Vanacker et al., 2019). In each watershed, one catena with a gentle slope and one with a steep slope were studied. On each catena, soil profiles were excavated at different positions along the slope (bottom, lower/upper middle, top), and soil samples were collected at multiple depths. For a selection of these samples ($n = 49$) both total elemental content and Fe-oxides (Fe_d, comprising Fe-oxides, -hydroxides and -oxihydroxides) with Dithionite-Citrate-Bicarbonate (DCB; Mehra and Jackson, 1958) were determined (for full laboratory procedures see Text A.1). This subset of samples was used as a calibration/validation dataset and is described in Table A1, Vanacker et al. (2019) and Fig. A1.

The total elemental content and Fe_d-measurements were used to calculate three weathering indices. The first one is the chemical index of alteration (CIA, dimensionless), which reflects the degree of weathering as the relative proportion of a conservative oxide, Al_2O_3, to the sum of the major oxides (CaO, Na_2O, K_2O) (Burke et al., 2007; Nesbitt and Young, 1982):

$$CIA = 100^*\left[\frac{Al_2O_3}{Al_2O_3 + CaO + Na_2O + K_2O}\right] \quad (1)$$

The CIA can be interpreted as a relative measure of the extent of the conversion of feldspar to clay, with associated leaching of the more labile oxides (Nesbitt and Young, 1982). High CIA-values therefore correspond to high chemical weathering degrees, with depletion of the base cations.

The total reserve in bases (TRB [$cmol_c\ kg^{-1}$]) is the sum of the total amount of alkaline and alkaline-earth elements (Ca^{2+}, Na^+, K^+, Mg^{2+}) (Delvaux et al., 1989; Herbillon, 1986):

$$TRB = Ca^{2+} + Na^+ + K^+ + Mg^{2+} \ \left[cmol_c\ \ kg^{-1}\right] \quad (2)$$

As mobile Ca, K, Mg and Na will be removed due to chemical weathering reactions, the TRB in soils will decrease with increasing weathering degree relative to the soil parent material if external inputs can be excluded.

As a third index, we used the ratio of DCB-extracted iron-oxides (Fe_d) to total iron (Fe_t), where DCB-extracted iron contains both crystalline and poorly crystalline iron oxides. As weathering advances, iron in primary minerals is released and becomes oxidized, hence the iron ratio (Fe_d/Fe_t, dimensionless) increases (Mehra and Jackson, 1958; Price and Velbel, 2003). A relatively limited Fe mobility is expected at our sites (Price and Velbel, 2003; Richter et al., 2009) given that i) these soils are not in saturated conditions (Robinet et al., 2018b, 2018a) where Fe reduction might favor the mobilization of colloidal carbon as Fe-organic carbon complexes (Buettner et al., 2014), and ii) Fe-oxides are not soluble in the pH_{H2O} range measured in our soils (5.16 ± 0.29 under forest and 5.69 ± 0.74 under cropland – Vanacker et al., 2019).

Weathering indices such as the CIA and TRB highly depend on the properties of the parent material (Garzanti et al., 2011; Price and Velbel, 2003). Therefore, bedrock samples were collected at 16 road cuts and quarries located in the study area (Fig. 1) and total elemental content was determined (see Text A.1). In absence of other spatially detailed geological and mineralogical information about the parent material, we used this sampling dataset to assert whether we could reasonably assume a relatively homogenous chemical composition of the parent material for the study area, as this might affect the chemical weathering degree of the soil.

2.3. Calibration/validation dataset: MIR spectroscopy and partial least square calibrations

The determination of chemical indices requires time-consuming and relatively costly chemical analysis (Section 2.2 Burke et al., 2007; Mehra and Jackson, 1958; Mohanty et al., 2016). A possible alternative is the use of techniques such as soil spectroscopy to rapidly assess soil weathering degree for a large number of samples at reduced cost. Soil spectroscopy has been used to estimate numerous soil properties such as organic matter, oxides, texture or exchangeable cations (Calderón et al., 2011; Cobo et al., 2010; Janik et al., 1998; Madari et al., 2006; Richter et al., 2009). However, few studies have investigated the application of soil spectroscopy for the determination of weathering indices (Baptista et al., 2011; Mohanty et al., 2016; Zhao et al., 2018).

The samples of the calibration/validation dataset for which the three weathering indices were measured (n = 49, Table A.1, Fig. A.1) were dried, sieved at 2 mm, crushed and scanned in the mid-infrared (MIR) region (FrontierTM with auto-sampler from PerkinElmer, Waltham, MA, USA). Five replicate samples were scanned from wavenumber 400 up to 4000 cm^{-1} at intervals of 1 cm^{-1} with 32 accumulations. To remove drifts from the signal, we scanned 5 KBr background samples every time before scanning the soil samples. We then divided the reflectance of the scanned samples by the average of the background samples. This procedure is similar to methodologies used by Reeves and Smith (2009), Calderón et al. (2011) or Forouzangohar et al. (2015).

In order to improve the data quality and the calibration, various pre-processing treatments were applied to the spectra which remove systematic variations caused by, for example, instruments or environmental conditions (Zeaiter et al., 2005) or by light scattering (Rinnan et al., 2009). The applied nine pre-processing treatments are the following:

i. moving average (Zeaiter et al., 2005)
ii. Savitzky-Golay filtering applied to the raw spectra (Savitzky and Golay, 1964)
iii. Savitzky-Golay filtering applied to the second derivative of the spectra (Savitzky and Golay, 1964)
iv. averaging of the first derivative (Stevens and Ramirez Lopez, 2014)
v. averaging of the second derivative (Stevens and Ramirez Lopez, 2014)
vi. multiplicative scatter correction (Geladi et al., 1985),
vii. standard normal variate (Barnes et al., 1989)
viii. standard normal variate – detrend (Barnes et al., 1989).
ix. raw specra (no pre-processing)

We used partial least squares (PLS) regressions to reduce the spectroscopic data of each sample to a limited number of factors. PLS is a commonly used method for multivariate calibration in quantitative spectral analysis (e.g. Bayer et al., 2012; Calderón et al., 2011). We limited the maximum number of factors to 20. We used PLS regressions of the spectral data directly against the weathering indices, and not against individual components of the indices. The different combinations of pre-processing treatments and numbers of PLS factors resulted in 180 PLS regressions for each weathering index. We divided our samples into a calibration sub-dataset (n = 32) and a validation sub-dataset (n = 17). To cover the whole range of values, we sorted the data in descending order and selected a validation sample every three measurements. We performed PLS regressions on the calibration sub-dataset.

We then used the validation sub-dataset to evaluate the best calibration for each predicted soil parameter. We evaluated the calibrations using the coefficient of determination (R^2) and the Akaike information criterion (AIC) that was calculated for the validation sub-dataset. The AIC evaluates the quality of models, considering both the goodness of fit and the degrees of freedom (Akaike, 1987). Here, we used the Sum of Squared Errors (SSE) as a measure of the goodness of fit and the number of PLS factors as a measure of the complexity of the models:

$$AIC = n^{*}\ln\left(\frac{SSE}{n}\right) + 2^{*}k \tag{3}$$

where n is the number of observations in the validation dataset and k the number of PLS factors. From all the possible combinations of pre-processing methods and number of PLS factors, we selected for each weathering index the combination yielding the lowest AIC. In order to verify the robustness of our calibration method the optimization procedure was repeated by using a leave-one-out cross-validation procedure.

2.4. Regional dataset: Site selection, soil sampling and calculation of weathering indices using MIR calibration relationships

Within the study area, we selected 50 forest and 50 agricultural sites (black and white circles Fig. 1a and Fig. A.1). We selected the forest sites manually based on Google Earth imagery. To avoid selecting newly forested sites, we evaluated satellite images from 2003 onwards and combined this information with field observations and surveys among the property owners. We adjusted our selection in order to cover the widest slope gradient range possible. To select the agricultural sites, we randomly distributed points over the whole study area. Based on Google Earth imagery, we relocated the points initially located in non-agricultural land to the nearest agricultural sites. We conducted surveys among the owners of the fields to evaluate the duration of agricultural activities at the agricultural sites. If it appeared that a site was converted from forest to arable land less than approximatively 30 years ago (which is the time span over which people could accurately recollect past land use), we replaced the site with a nearby older site. The assumption that initial soil thicknesses were identical under forested and agricultural sites is discussed in Text A. 2.

At each selected site, we identified a position on a linear slope located approximately at the middle of the catena (referred to as mid-slope position in the remainder of the text) in order to be able to compare between sites. We measured the position with a handheld GPS (Garmin Etrex Venture HC, horizontal and vertical accuracies of approximatively 3 m). At each identified position, we augered the soil down to the saprolite layer or to a maximum depth of 3 m using an Edelman auger (Eijkelkamp Soil & Water, Giesbeek, The Netherlands). Soil horizons were delimited and described according to the FAO guidelines (Jahn et al., 2006). We collected ca. 100 g of soil from each horizon from the core of the auger in order to avoid contamination. Samples were air-dried at 40 °C and gently crushed and sieved at 2 mm to obtain the fine earth fraction.

We measured the MIR reflectance of the regional soil samples following the same procedure as for the calibration/validation samples (Section 2.3), and applied the best calibration relationships (the pre-processing method and number of PLS factors yielding the lowest AIC) to derive estimates of the weathering indices. In the remainder of the text we refer to these weathering degrees as the *estimated* CIA, TRB and Fe_d/Fe_t. Values determined in the lab are referred to as *measured*. The possible implications of applying the catena-scale MIR calibration relationships to the regional dataset are discussed in Text A.3. Text A.4 provides details on the uncertainty determination of the estimated weathering index-values.

2.5. Identification of factors explaining the spatial variability of soil thickness and weathering degree

For each regional sampling site, we also measured a series of environmental factors that potentially explain the spatial variability of soil thickness and chemical weathering degree. We classified the land use of each site as either forest or agricultural. Soil thickness was measured vertically from the surface to the soil-saprolite interface, which was identified by using color (white to light yellow) and texture (loose, coarse grained sandy material) as morphological indicators, or to a maximum depth of 3 m. The slope was measured in the field with a clinometer and we extracted the elevation and the distance to the drainage divide from the 30 m resolution DEM of the NASA Shuttle Radar Topographic Mission (SRTM, Farr et al., 2007). We did not account for possible variations in climatic conditions, but given the limited size of the study area we may assume that such variations are negligible.

We used Pearson correlation coefficients (r) and stepwise linear regressions to evaluate and identify relationships between the soil thickness, weathering indices and explaining factors. In the stepwise linear regression land use was included as a binary independent variable (forest = 1, agriculture = 0). Variables were added to the model when the F-statistic was less than the significance level ($p < 0.05$). Since the data were not-normally distributed we used the Wilcoxon rank sum test for assessing the effect of land use at a significance level of 0.05. For each estimated weathering index, we investigated these relationships for i) the full dataset containing all depth-samples at each location ($n = 229$, Table A.2) and ii) one depth averaged value for each sampling location ($n = 96$, Table A.3) summarized in Fig. A.1.

3. Results

3.1. Calibration of MIR spectral reflectance with weathering indices

The average R^2 of the PLS regressions between the weathering indices and the MIR spectral reflectance for all considered pre-processing methods and number of PLS components combinations is 0.81, 0.66 and 0.58 for the CIA, TRB and Fe_d/Fe_t, respectively. Pre-processing methods that use derivatives of the spectral signal often result in a lower R^2 for similar AIC values compared to the other pre-processing methods (not shown). All the other methods present similar R^2 and AIC values. Compared to the CIA and the TRB, the PLS calibration for Fe_d/Fe_t systematically yields a lower R^2 (Table 1). For each weathering index, we selected the combination of pre-processing method and number of PLS factors yielding the lowest AIC, both for the method with the sorted values and leave-one-out cross-validation. Both methods yield almost identical results with an equally high predictive power (Table 1). The identified optimal calibration method for the sorted values is applied to the regional dataset.

Table 1
Calibration results of the 49 soil samples of the calibration/validation dataset for which all weathering indices were measured (Table A.1, Fig. A.1). Three weathering indices (chemical index of alteration (CIA), total reserve in bases (TRB) and iron ratio (Fe_d/Fe_t)) were calibrated with the MIR spectral signal based on partial-least squares (PLS) regressions. The best combination of pre-processing method with number of PLS factors was selected based on the lowest Akaike information criterion (AIC) and root mean squared error (RMSE) and highest coefficient of determination (R^2) value of the validation samples. "DT" and "MSC" stand for Standard Normal Variate – Detrend (Barnes et al., 1989) and Multiplicative Scatter Correction *(*Geladi et al., 1985*)*, respectively. Both the results of the calibration method using the sorted values and leave-one-out cross-validation procedure are shown, where the optimal method as identified by the sorted values is applied to the regional dataset.

Index	Pre-processing	# of PLS factors	R^2	AIC	RMSE
Sorted values					
CIA	DT	6	0.97	29.51	1.67
TRB	MSC	7	0.91	87.02	8.56
Fe_d/Fe_t	DT	3	0.84	−96.9	0.048
Leave-one-out cross-validation					
CIA	DT	7	0.95	81.02	1.96
TRB	MSC	6	0.93	211.51	7.58
Fe_d/Fe_t	DT	5	0.80	−287.59	0.05

From the 50 forest sites, no samples could be collected at 4 of them due to the absence of soil (F34, F35, F40 and F47 - Table A.2). As a result, the final dataset contains a total of 229 samples from 46 sites under forest and 50 sites under agricultural land use (Fig. A.1). The number of soil horizons sampled is similar for forest sites (2.4 ± 1.3) and agricultural sites (2.5 ± 1.5). The selected optimal PLS regression models using the sorted values (Table 1) were used to estimate the weathering indices for each regional sample. The range of the estimated weathering indices values is similar to the range present in the measured calibration/validation dataset (Table A.1, Table 2). The standard deviation of the estimated weathering indices of the regional dataset (Table 2) is roughly a factor 4 larger than the uncertainty of the estimated weathering indices, represented by the RMSE between estimated and measured weathering indices (Table 1). This means that the PLS regression models are sufficiently accurate to represent the spatial variation of weathering indices in the regional dataset. The standard deviations of the residuals increase with increasing values of TRB and decreasing values of the CIA and Fe_d/Fe_t (Fig. A.2). The calculated CIA values for six highly weathered samples are higher than 100 and seven calculated TRB values are negative, which is physically impossible (Table A.2). Therefore these values were set to the physically possible upper and lower limit (0–100 for the CIA and >0 for the TRB). These values are most likely a consequence of the extrapolation of the PLS calibration relationships to regional samples that have values outside of the range considered in the original calibration. There is a good correlation between the estimated CIA, TRB and Fe_d/Fe_t, which is higher for the depth averaged values compared to the full dataset (Table 2).

3.2. Spatial variations in total elemental composition of the parent material

SiO_2 dominates the measured total elemental composition of the bedrock samples collected throughout the study area (Table 3). We observe a SiO_2 content of 63.75 ± 8.22% on average, while the samples contained on average 12.64 ± 0.63% Al_2O_3 and 7.97 ± 3.79% of Fe_2O_3. The majority of the bedrock samples (75%) has a SiO_2 composition ranging between 64 and 73%, with Na_2O and K_2O accounting for 4.5 to 8% of the total elemental content. These values are typical for an intermediate to felsic magmatic composition or rhyodacite parent material (Le Bas and Streckeisen, 1991). Four samples have a remarkably lower SiO_2, Na_2O and K_2O content (B-4, B-11, B-12 and B-13, Table 3), with a corresponding increase in the relative proportion of Fe_2O_3 and MgO, denoting the ferromagnesian character of the bedrock, likely of basaltic nature (Le Bas and Streckeisen, 1991). Three of these samples with high Fe-concentrations also contain significant amounts of CaO. Clearly, local variations in bedrock composition are present in our sampling region. These variations could not be related to variations in surface elevation and are therefore likely related to local variations in the elevation of the basalt-rhyodacite contact (Fig. A.3).

3.3. Impact of LUCC on soil thickness and weathering degree

Soils are slightly, but significantly, thicker at the mid-slope position for agricultural sites (121.96 ± 92.64 cm) compared to forest sites (85.02 ± 74.90 cm, p-value = 0.02 - Fig. 2) when confounding factors are not accounted for. While we sampled forest hillslopes with slope gradients up to 41° (16.4 ± 10.8°), the steepest gradient measured at the agricultural sites was only 34° (14.2 ± 8.3° - Table A.2). Mean slope gradients for both land uses are, however, not significantly different (p-

Table 2
Descriptive statistics and Pearson correlation coefficients (r) for the estimated weathering indices (chemical index of alteration (CIA), total reserve in bases (TRB [$cmol_c$ kg^{-1}]) and iron ratio (Fe_d/Fe_t)) and the measured explaining factors used in the analysis for i) the full dataset containing all samples and ii) a depth averaged value for each sampling location.

Dataset	Variables	# samples	Mean	Std	Min	Max	Pearson correlation coefficients						
							CIA	TRB	Fe_d/Fe_t	ln(Soil thickness)	Slope gradient	Elevation	Distance to divide
							[-]	[$cmol_c$ kg^{-1}]	[-]	[ln(cm)]	[°]	[m]	[m]
All soil samples	CIA	229	88	9	62	100		−0.81	0.50	0.57	−0.60	0.45	−0.12
	TRB	229	58	35	0	162	−0.81		−0.72	−0.54	0.67	−0.53	0.12
	Fe_d/Fe_t	229	0.54	0.11	0.18	0.99	0.50	−0.72		0.28	−0.37	0.25	−0.14
	ln(Soil Thickness)	100	4.74	0.79	2.20	5.70	0.57	−0.54	0.28		−0.66	0.34	0.04
	Slope gradient	100	11.5	8.0	2.5	41.0	−0.60	0.67	−0.37	−0.66		−0.55	0.04
	Elevation	100	676	75	417	771	0.45	−0.53	0.25	0.34	−0.55		−0.30
	Distance to divide	100	151	91	0	437	−0.12	0.12	−0.14	0.04	0.04	−0.30	
Depth averaged	CIA	96	85	10	62	100		−0.91	0.73	0.67	−0.72	0.51	−0.26
	TRB	96	70	37	0	161	−0.91		−0.79	−0.62	0.73	−0.53	0.22
	Fe_d/Fe_t	96	0.53	0.10	0.25	0.87	0.73	−0.79		0.40	−0.52	0.25	−0.21

Table 3
Measured % oxides of the major total elements for all bedrock samples collected throughout the study area (red triangles Fig. 1). The elevation [m] of the sampling location is also indicated. The total reserve in bases (TRB [$cmol_c$ kg^{-1}]) and chemical index of alteration (CIA) are calculated for all bedrock samples, as well as their mean and standard deviation (std.).

Bedrock sample	Al_2O_3	Fe_2O_3	CaO	K_2O	MgO	Na_2O	MnO	P_2O_5	SiO_2	TiO_2	Elevation	TRB	CIA
	[%]	[%]	[%]	[%]	[%]	[%]	[%]	[%]	[%]	[%]	[m]	[$cmol_c$ kg^{-1}]	
B-1	14.16	6.73	0.24	3.44	0.40	1.13	0.08	0.19	66.05	0.83	747	182	75
B-2	12.14	5.45	1.18	4.35	0.70	2.31	0.13	0.20	67.70	0.70	753	328	61
B-3	12.08	5.70	1.49	4.23	0.52	2.70	0.08	0.18	68.78	0.69	675	343	59
B-4	13.47	13.02	9.61	0.71	5.82	2.15	0.19	0.12	46.63	1.27	632	1070	52
B-5	12.26	6.10	1.43	4.27	0.54	2.70	0.10	0.18	67.87	0.66	556	342	59
B-6	12.28	5.10	0.29	6.28	0.31	1.74	0.05	0.11	69.56	0.65	491	277	60
B-7	12.93	7.51	2.52	3.57	0.79	3.10	0.10	0.33	63.83	1.08	586	417	58
B-8	12.44	5.44	1.06	4.74	0.32	2.53	0.09	0.19	70.05	0.67	686	311	60
B-9	11.88	5.21	0.46	4.34	0.66	1.68	0.06	0.02	67.54	0.70	494	262	65
B-10	12.12	5.90	0.93	5.10	0.61	1.18	0.04	0.18	72.17	0.77	797	278	63
B-11	12.41	14.02	6.44	1.98	2.94	2.56	0.20	0.31	53.13	1.69	648	725	53
B-12	12.97	14.48	7.94	1.36	4.30	2.70	0.24	0.18	50.79	1.56	658	902	52
B-13	12.55	15.28	1.75	1.48	1.43	0.39	0.28	0.32	51.33	1.88	524	260	78
B-14	12.46	5.82	0.74	5.11	0.26	2.09	0.05	0.19	69.03	0.66	473	280	61
B-15	13.61	5.99	0.10	4.68	0.38	1.44	0.12	0.14	66.44	0.79	557	219	69
B-16	12.43	5.70	0.32	4.53	0.52	1.64	0.08	0.07	69.15	0.74	343	246	66
Mean	12.64	7.97	2.28	3.76	1.28	2.00	0.12	0.18	63.75	0.96	601	403	62
Std.	0.63	3.79	2.96	1.57	1.63	0.73	0.07	0.08	8.22	0.41	121	260	7

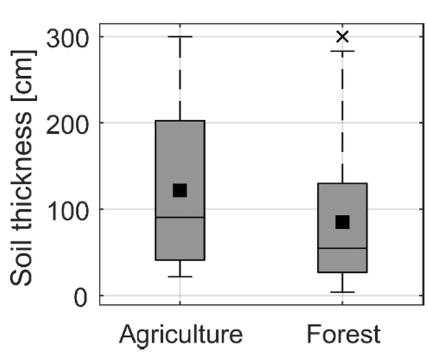

Fig. 2. The measured soil thickness at the mid-slope position is significantly higher for agricultural sites (121.96 ± 92.64 cm) compared to the forest sites (85.02 ± 74.90 cm, p-value = 0.02) when not accounting for confounding factors. Mean values are indicated by the black squares.

value = 0.44). The agricultural sites are overall located at lower altitudes than the forest sites (631.4 ± 93.5 and 678.1 ± 75.3 m, respectively), and show a longer distance to the nearest catchment divide (165.8 ± 88.6 and 141.2 ± 89.9 m, respectively).

Soil weathering degree shows small, non-significant, differences for the CIA (87 ± 10 and 89 ± 8, p-value = 0.07), TRB (60 ± 35 and 58 ± 34 $cmol_c$ kg^{-1}, p-value = 0.85) and Fe_d/Fe_t (0.54 ± 0.13 and 0.55 ± 0.09, p-value = 0.99 - Fig. 3) between forest and agricultural land when considering the full dataset, again when we do not account for possible confounding factors. Similarly, non-significant differences are observed when using the depth averaged values (Fig. A.4).

3.4. Relations between soil thickness and explaining factors

The slope gradient, the elevation, and the distance to the nearest catchment divide measured at the different sampling sites all cover a wide range of values (Table 2). A strong negative non-linear relationship is observed between the measured soil thickness and slope gradient, both for forest and agricultural sites (r = -0.66 – Table 2, Fig. 4a). Less explicit is the correlation between soil thickness and elevation (r = 0.34 – Table 2, Fig. 4b), which at least partially results from the high

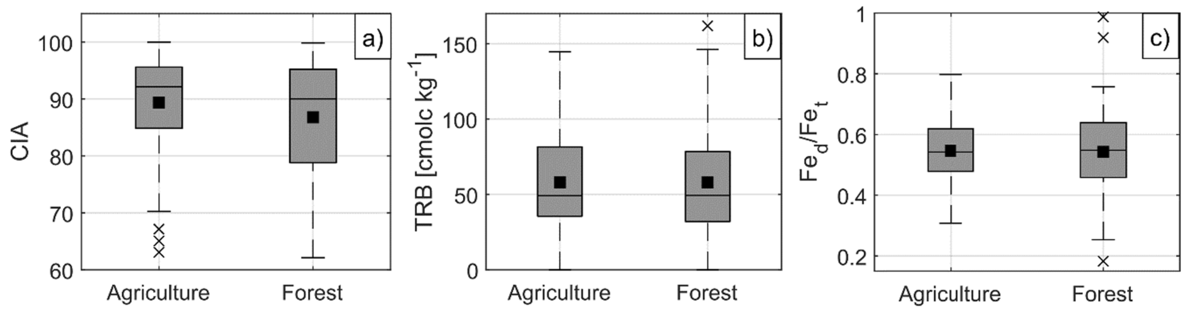

Fig. 3. Weathering degree under agriculture and forest at the mid-slope position for the full dataset (all soil horizons) determined by the estimated a) chemical index of alteration (CIA [-]), b) total reserve in bases (TRB [$cmol_c$ kg^{-1}]) and c) iron ratio (Fe_d/Fe_t [-]). No significant differences between both land use types were observed (p-values of 0.07, 0.85 and 0.99 for the estimated CIA, TRB and Fe_d/Fe_t, respectively). Black squares indicate the mean value.

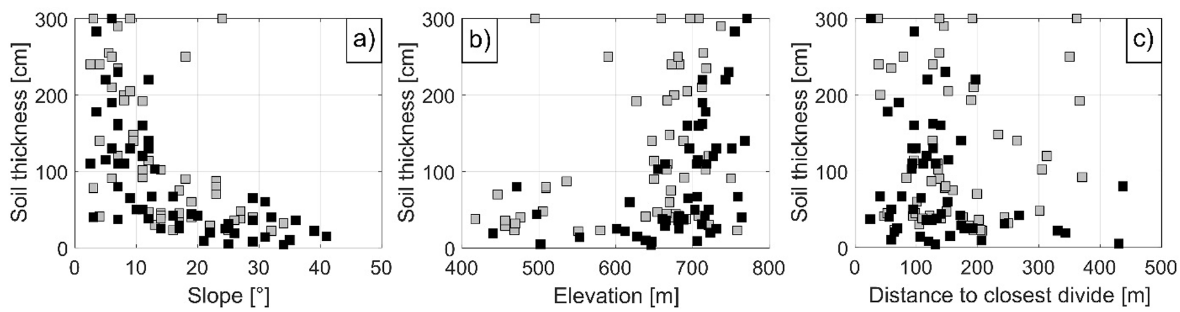

Fig. 4. Measured soil thickness versus measured potentially explaining factors at the mid-slope position: a) Slope gradient [°], b) Elevation [m] and c) Distance to the closest drainage divide [m]. Both forest sites (black) and agricultural sites (grey) are shown, following similar trends.

correlation between slope gradient and elevation (r = -0.55 – Table 2): thick soils are generally found on gentle slopes at a higher elevation. Soil thickness is only poorly related to the distance to the closest divide (r = 0.04 – Table 2, Fig. 4c).

A stepwise linear regression was performed to identify the relative importance of the explaining factors on the spatial variations in soil thickness, where land use was included as a binary independent variable (forest vs. agriculture). A log transformation was applied to the soil thickness, given the non-linear relationship between soil thickness and explaining factors (Fig. 4).

Table 4
Results of the stepwise linear regressions for the measured soil thickness and the three estimated weathering indices (chemical index of alteration (CIA), total reserve in bases (TRB [$cmol_c$ kg^{-1}]) and iron ration (Fe_d/Fe_t)) at the mid-slope position for the whole dataset (n = 229) and the depth averaged value (n = 96). The "t-statistic" corresponds to the F-test on the coefficient estimate. The "Order" corresponds to the order of inclusion in the stepwise linear regression models (significance level p < 0.05).

Dataset	Index	R^2	Variables	Estimate	Standard Error	t-statistic	p-value	Order	R^2	RMSE
	Ln (Soil thickness)	0.53	Intercept	5.52E + 00	1.37E-01	4.03E + 01	3.26E-63	0	0	0.98
			Slope gradient	−7.29E-02	7.08E-03	−1.02E + 01	2.57E-17	1	0.5	0.70
			Land use (Forest)	−3.67E-01	1.34E-01	−2.74E + 00	7.25E-03	2	0.53	0.70
All soil samples	CIA	0.48	Intercept	5.99E + 01	7.18E + 00	8.34E + 00	7.63E-15	0	0.00	9.26
			Slope gradient	−3.26E-01	8.33E-02	−3.92E + 00	1.18E-04	1	0.37	7.39
			Ln(Soil thickness)	3.22E + 00	7.64E-01	4.22E + 00	3.61E-05	2	0.42	7.09
			Elevation	3.03E-02	8.08E-03	3.75E + 00	2.29E-04	3	0.44	6.97
			Land Use (Forest)	−4.14E + 00	1.01E + 00	−4.08E + 00	6.34E-05	4	0.47	6.77
			Distance to divide	−1.13E-02	5.31E-03	−2.13E + 00	3.39E-02	5	0.48	6.72
	TRB	0.51	Intercept	1.44E + 02	2.47E + 01	5.85E + 00	1.71E-08	0	0.00	34.73
			Slope gradient	1.87E + 00	3.02E-01	6.18E + 00	2.91E-09	1	0.46	25.69
			Elevation	−1.06E-01	2.58E-02	−4.10E + 00	5.79E-05	2	0.49	24.90
			Ln(Soil thickness)	−7.69E + 00	2.73E + 00	−2.81E + 00	5.33E-03	3	0.51	24.53
	Fe_d/Fe_t	0.15	Intercept	6.27E-01	1.65E-02	3.80E + 01	4.90E-100	0	0.00	0.11
			Slope gradient	−5.13E-03	8.68E-04	−5.91E + 00	1.27E-08	1	0.14	0.11
			Distance to divide	−0.00016	7.69228E-05	−2.0336183	0.0431587	2	0.15	0.11
Depth averaged	CIA	0.61	Intercept	7.90E + 01	5.32E + 00	1.49E + 01	4.64E-26	0	0.00	9.71
			Slope gradient	−4.57E-01	9.12E-02	−5.02E + 00	2.58E-06	1	0.51	6.86
			Ln(soil thickness)	3.84E + 00	9.76E-01	3.94E + 00	1.61E-04	2	0.56	6.48
			Distance to divide	−2.29E-02	7.11E-03	−3.22E + 00	1.76E-03	3	0.61	6.14
	TRB	0.60	Intercept	1.45E + 02	3.21E + 01	4.51E + 00	1.95E-05	0	0.00	37.40
			Slope gradient	1.75E + 00	3.91E-01	4.48E + 00	2.17E-05	1	0.53	25.87
			Elevation	−9.05E-02	3.24E-02	−2.79E + 00	6.37E-03	2	0.57	24.55
			ln(Soil thickness)	−9.58E + 00	3.79E + 00	−2.53E + 00	1.33E-02	3	0.60	23.86
	Fe_d/Fe_t	0.25	Intercept	6.01E-01	1.52E-02	3.94E + 01	7.39E-60	0	0.00	0.10
			Slope gradient	−4.96E-03	8.51E-04	−5.82E + 00	8.15E-08	1	0.25	0.09

The main factor explaining variations in soil thickness is the slope gradient ($R^2 = 0.50$ – Table 4). Adding land use only slightly improves the predictive power of the fitted relationship ($R^2 = 0.53$ – Table 4).

3.5. *Relations between soil weathering degree and explaining factors*

The CIA and the TRB have overall stronger relationships with the explaining factors compared to the Fe_d/Fe_t (Table 2). The slope gradient most strongly correlates with the estimated weathering indices (whereby weathering degree is negatively related to slope gradient). All weathering indices have a weak correlation with the distance to the closest catchment divide, suggesting that a higher distance from the divide is associated with a somewhat lower weathering degree. All three indices have the highest correlations with the logarithm of the soil thickness (with thicker soils being more weathered) and the slope gradient (with gentle slopes being more weathered). Pearson correlation coefficients are in general ca. 0.1 higher when considering the depth averaged values compared to the full dataset for all explaining factors (Table 2). Scatter plots of the different environmental factors versus the weathering indices highlight the strong, non-linear relationships between weathering degree and soil thickness, especially for the CIA and the TRB (Fig. 5). This non-linearity between weathering degree and soil thickness is absent for Fe_d/Fe_t and the correlation is weaker (Fig. 5, Table 2).

The stepwise linear regression results in higher R^2 for the CIA (0.48) and the TRB (0.51) compared to Fe_d/Fe_t (0.15) when considering all samples. Similarly, the highest R^2-values are obtained for the CIA (0.61) and TRB (0.60) compared to Fe_d/Fe_t (0.25) when using one depth averaged value per sampling location (Table 4), which results in a higher explanatory power compared to the full dataset. The remaining RMSE of the linear regressions is for all indices higher than the RMSE associated with the estimation uncertainties (Table 1 and 4). This indicates that

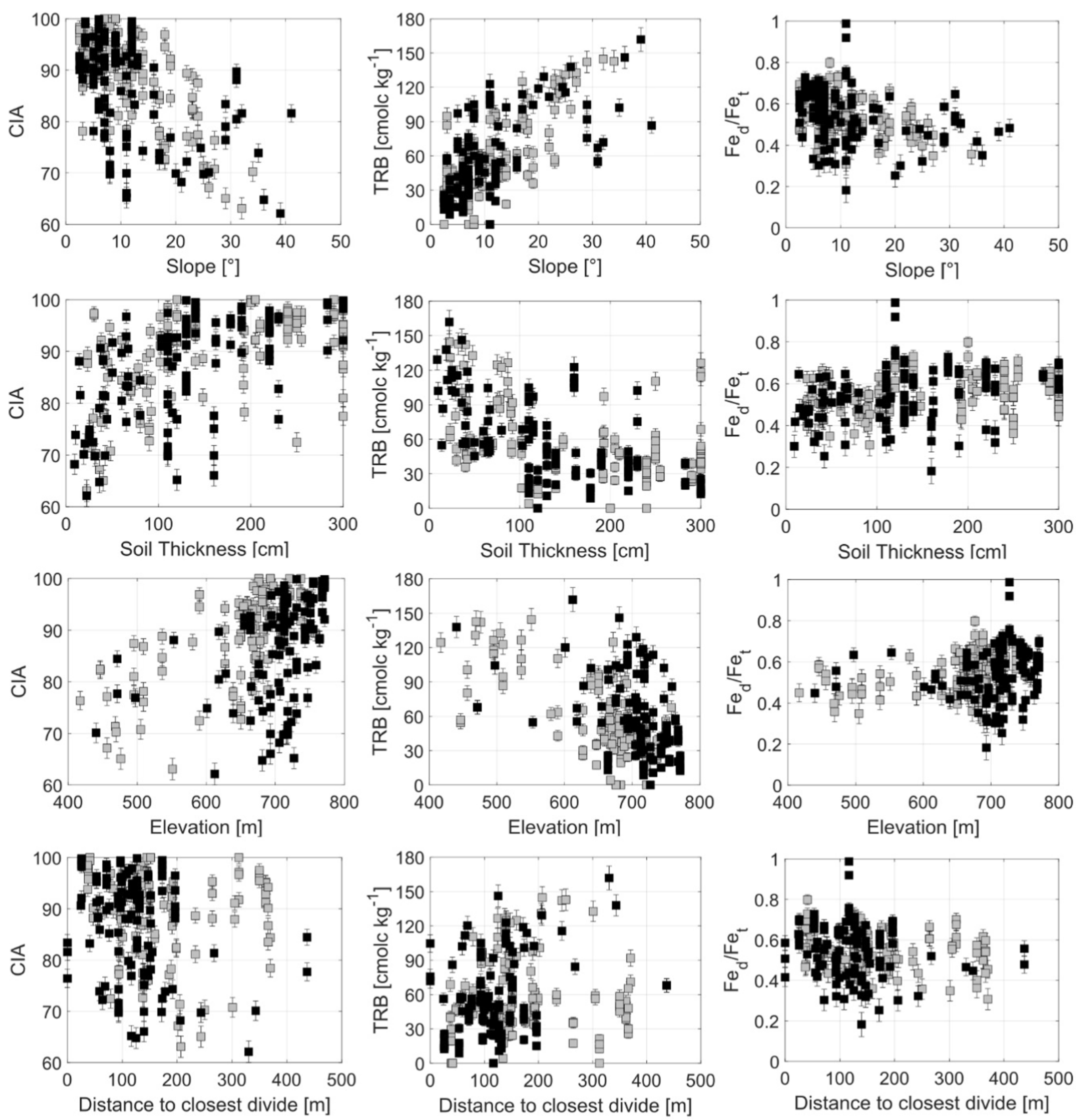

Fig. 5. Estimated chemical index of alteration (CIA), total reserve in bases (TRB [$cmol_c\ kg^{-1}$]) and iron ratio (Fe_d/Fe_t) at the mid-slope position versus the measured explaining factors investigated in this study: row 1) slope gradient [°], row 2) soil thickness [cm], row 3) elevation [m] and row 4) distance to closest divide [m]. Both forest sites (black) and agricultural sites (grey) are shown. Error bars show the uncertainty on the estimated values, which was determined from the standard deviation on the moving average of the residuals between the estimated and measured values of the calibration/validation dataset (Fig. A.2).

variations of the residuals between the weathering degrees predicted by the stepwise linear regression model and the estimated weathering degrees are larger than the uncertainty of the weathering degrees estimated from MIR spectra.

The slope gradient is always the first variable included in the stepwise linear regression model, both when using all samples and one depth averaged value per sampling location. Successive addition of other factors only results in a minor, yet significant, increase of the respective R^2 (Table 4). The higher R^2-values when using the depth averaged dataset all result from the increase in explanatory power of the slope gradient, where the other explanatory variables are of the same magnitude as when considering the full dataset. This shows that variations in weathering degree throughout depth are much smaller than variations between slope gradients. As more weight is attributed to sampling locations with thicker soils when considering the full dataset, this results in a lower explanatory power of the model when compared to the depth averaged values where an equal weight is attributed to each sampling location.

Soils under agricultural land are slightly thicker in comparison to soils under forest, but land use only explains ca. 3% of the total variance when the effect of slope gradient is accounted for (Table 4). Soil thickness and elevation are both positively related to weathering degree, after accounting for the slope effect, each explaining an additional 2–5% of the variance of the CIA and TRB, both when considering all samples and one depth averaged value per sampling location (Table 4). Land use is only significantly related to the calculated CIA when considering all samples, suggesting that forest soils are slightly less weathered. As is the case for soil thickness, land use explains only a small part of the variance in CIA values (3%) (Table 4).

4. Discussion

4.1. Successful use of MIR spectroscopy to infer soil weathering indices

The use of PLS regressions allowed us to establish calibration relationships between the MIR spectral reflectance and weathering indices of the soil samples (Table 1). The quality of these calibrations are similar to the results of Mohanty et al. (2016), who also related weathering indices to spectral reflectance. Our results are also in the same range as those obtained when predicting the concentrations of the individual chemical elements used in weathering indices (Nocita et al., 2015; Soriano-Disla et al., 2014). The concentration of Al_2O_3, the immobile constituent of the CIA index, was already successfully predicted using the combination of PLS with MIR spectroscopy by Janik et al. (1995) and Bertrand et al. (2002). For the other major oxides considered in the CIA calculation both poorer predictions (Janik et al., 1995) and predictions of similar quality (Janik et al., 1998) were reported. Several studies already showed the potential of MIR reflectance analysis to predict exchangeable cations, including exchangeable Ca, Mg, K and Na (Cobo et al., 2010; Janik et al., 1995; Minasny et al., 2009; Pirie et al., 2005; Soriano-Disla et al., 2014). Exchangeable Na and K sometimes showed lower correlations, probably due to narrow ranges and low concentrations (Janik et al., 1998; Minasny et al., 2009; Pirie et al., 2005). In our TRB calculations we used the total cation content of the samples, i.e., not only the exchangeable cations but also the cations locked into the primary and secondary minerals. It seems therefore that MIR reflectance can be used to quantify not only the exchangeable cations, but also the total cation content. The reasonably good prediction of the Fe_d/Fe_t also corresponds well with results from the literature (Bertrand et al., 2002; Janik et al., 1995, 1998; Reeves and Smith, 2009).

Our study thus supports the use of MIR as a tool for the rapid assessment of a large quantity of chemical soil properties. We could not directly identify the reason(s) for the slightly lower R^2 obtained for Fe_d/Fe_t in comparison to the CIA and the TRB (Table 1). Some studies observed weaker and fewer Fe-oxide absorption bands in the MIR region compared to the NIR region (Richter et al., 2009; Soriano-Disla et al., 2014). Richter et al. (2009) also observed an impact of soil texture on the predictive power of visible and near infrared reflectance (VIS-NIR region) for the prediction of Fe-oxides, where variations in the clay and silt fraction were altering the predictive results.

4.2. Potential impact of lithological variations

Lithological variation between sampling sites is a potential source of error as it might change the baseline of the different soil weathering indices. In our study area, two major lithologies compose the parent material. Basalt is reported to be found at lower altitudes, while rhyodacite is often found on top of the basalt at higher altitudes (Bellieni et al., 1986; Ernesto et al., 1990; Renne et al., 1992). The analysis of the bedrock samples we collected throughout the study area showed that there was indeed important variation in their elemental compositions. Two clusters could be distinguished (Table 3, Fig. A.3). 75% of the bedrock samples had a composition that reflects an intermediate to felsic magmatic composition, typical for rhyodacitic material (Le Bas and Streckeisen, 1991). Four bedrock samples (25%), however, showed a deviating composition, characterized by lower SiO_2 contents of 47 to 53%, indicating a basaltic rock type. The absence of a relationship between SiO_2 and the elevation at which the samples were collected (Fig. A.3.) indicates that variations in lithology are not necessarily linked to altitude or landscape position: they may be due to variations in altitude of the basalt-rhyodacite contact related to the basaltic topography that was covered by the later rhyodacitic outflows.

Variations in lithology will mainly affect the CIA and TRB, as different parent materials will result in different 'baseline' values. The TRB reflects the extent of removal of alkaline and alkaline-earth cations throughout the weathering processes, where the base value depends on the composition of the bedrock material. We calculated the TRB for the bedrock samples. The samples characterized by a basaltic signature (B-4, B-11, B-12 and B-13) have a mean TRB of 739 ± 349 $cmol_c\ kg^{-1}$, which is significantly higher (p-value = 4.5e-4) than the TRB of the rhyodacitic samples (290 ± 63 $cmol_c\ kg^{-1}$ – Table 3). No significant difference was found between the CIA of the basaltic (59 ± 13) and rhyodacitic (62 ± 5) samples (p-value = 0.17). In contrast to the CIA and TRB, the iron ratio is, in principle, not sensitive to lithological heterogeneities, as it is a relative measure of the degree of oxidation.

The TRB values we measured and calculated for our soil samples range from 0 to 161 $cmol_c\ kg^{-1}$ and are all well below the average value we obtained for rhyodacitic bedrock. Therefore, we were not able to clearly distinguish basalt-derived soil samples in our dataset. The latter is not surprising: lateral soil transport is important in this landscape and the soils found at the mid-slope section do contain material derived from the entire bedrock sequence upslope of the mid-slope point, thereby averaging out to some extent possible variations in bedrock composition (Brosens et al., 2020). Thus, while bedrock variability certainly cannot explain the patterns we found in the data, it almost certainly contributed significantly to the ca. 40 to 50% of variation in soil weathering degree that we cannot explain using the variables we measured (Table 4).

4.3. Slope gradient as a major control on soil thickness and weathering degree

4.3.1. Impact on soil thickness

Slope gradient is the main factor explaining the regional variations in soil thickness at the mid-slope position (Table 2 and 4). Soil thickness decreases exponentially with increasing slope gradient (Fig. 4a), which can be explained by the changing equilibrium soil thickness that depends on the balance between erosion and weathering on the one hand and soil production on the other hand, where erosion rates are higher on steeper slopes (see Text A.5 and Brosens et al., (2020)). Soil thickness varies widely for slopes smaller than approximately 15° (Fig. 4a). Local variations in bedrock mineralogy and/or jointing patters and location-specific hydrological conditions are likely to be important in controlling local weathering rates and hence soil thickness on lower slope gradients. At steeper slopes the effect of such local variations is overwhelmed by the high lateral soil flux (Brosens et al., 2020).

4.3.2. Impact on soil chemical weathering degree

Slope gradient is also strongly related to the CIA and the TRB and to a lesser extent to Fe_d/Fe_t (Table 2 and 4, Fig. 5). These regional observations are consistent with the analysis carried out by Vanacker et al. (2019) at the catena-scale: on two steep slope transects clear spatial variations in weathering degree along the slope could be observed (with a decrease in weathering degree with increasing slope gradient), which were absent for both gentle sloping transects that were analyzed. The coupling between soil weathering degree and slope gradient is again related to increased soil erosion processes on steeper slopes, leading to more rapid soil rejuvenation and the exposure of less weathered soil material at steeper, faster eroding, sites which is further examined and discussed in Brosens et al. (2020).

The CIA and the TRB were not only strongly linked with slope gradient, but also to soil thickness whereby thicker soils were more weathered, which explains an additional 2–5% of the variance in weathering degree (Table 2, Fig. 5). The presence of a thicker soil on a given slope can be seen as an indication of a longer soil residence time, which can be expected to result in a higher weathering degree (Brosens et al., 2020). Also elevation explains a small additional fraction of the variance in weathering degrees when slope gradient is accounted for (Table 4). Previous studies showed that elevation can be related to soil weathering, notably through changes in climatic regimes with altitude (Dixon et al., 2009; Rasmussen et al., 2011). The somewhat higher rainfall amounts at higher altitudes (daily rainfall is ca. 30% higher at 800 m compared to 400 m a.s.l.) that have been observed in the south of Rio Grande do Sul (Damé et al., 2016) might therefore explain this small effect.

We could not identify the exact mechanism explaining the weaker association between the explaining variables for Fe_d/Fe_t compared to the CIA and TRB (Tables 2 and 4, Fig. 5). A first possible reason could be error-propagation due to the lower predictive power of the PLS calibrations between the MIR spectral reflectance and Fe_d/Fe_t (R^2 of 0.84, Table 1). Another reason could be related to the inherent properties of the weathering indices considered. The CIA and the TRB are based on the mobility of major cations, while Fe_d/Fe_t measures the formation of secondary minerals. Possibly such mineral formation processes reach an equilibrium value over a time scale that is longer than the soil residence time on the hillslope that we observed. Alternatively, if iron oxidation proceeds rapidly, no variations in Fe_d/Fe_t will be observed because the ratio will be close to its maximum for all samples. Given the relatively high values of Fe_d/Fe_t that we observed (exceeding 0.4 for nearly all samples) the latter hypothesis appears to be the more likely. Accounting for poorly-crystallized oxalate-extractable iron oxides (Fe_o) and using $(Fe_d\text{-}Fe_o)/Fe_t$ as a measure of the weathering intensity might also improve the calibration and correlation-results (Baumann et al., 2014; Baumler, 2004). We did not observe a general trend in weathering degree with depth (not shown). However, we did observe significantly higher CIA values in the subsoil when compared to the topsoil, both under forest and agriculture. This difference was not apparent for the TRB or Fe_d/Fe_t (Fig. A.5). The higher CIA values in the subsoil are likely caused by a relative increase in Al_2O_3 with depth, which, however, does not hamper the use of the CIA which continues to express relative differences in weathering degree (see Text A.6).

4.4. Absence of clear LUCC impact on soil thickness and weathering degree

4.4.1. Soil thickness

The absence of an important land use effect on soil thickness is, at first sight, surprising. ^{137}Cs measurements in the 1.19 km^2 Arvorezinha catchment, which is located in the study area, showed high rates of erosion and deposition along hillslope transects with losses averaging 42 t ha^{-1} yr^{-1} for erosional sites and deposition rates averaging 29 t ha^{-1} yr^{-1} for depositional sites on hillslope profiles (Minella et al., 2014). Such erosion rates would lead to important changes in soil thickness over a timescale of several decades. Several factors may explain this apparent contradiction. The ^{137}Cs measurements do indeed show important soil movement, but soil losses were not maximum on the steepest hillslope positions (as one would expect when water erosion is dominant), but at top and shoulder positions (Minella et al., 2012, 2014). Furthermore, important deposition was sometimes observed on intermediate slope positions and on rather steep foot-slopes. Such an erosion–deposition pattern is typical for a diffusive process such as tillage erosion. Tillage will cause intensive redistribution of soil within a field whereby erosion takes place on convexities and downslope of field borders and deposition will occur in concavities and upslope of field borders (Van Oost et al., 2006). Local erosion rates induced by tillage erosion can be very high (>30 t ha^{-1} yr^{-1}) and associated deposition rates can exceed 100 t ha^{-1} yr^{-1} but, importantly, tillage erosion does only redistribute soil within a field parcel and will have no effect on soil thickness on rectilinear slope segments, no matter what the slope gradient is (Van Oost et al., 2006). Thus, high erosion and sedimentation rates may occur within a field, while soil thickness on the mid-slope section of steep slopes remains stable when tillage erosion is causing soil movement.

However, Minella et al. (2014) also observed deposition of over 1 m of sediment on nearly flat areas, which cannot be attributed to tillage erosion, and calculated gross erosion on arable land was significantly higher than calculated gross deposition (977 t yr^{-1} vs. 540 t yr^{-1}). Assuming that, on average, 50% of soil movement is due to water erosion, water erosion on arable land would total ca. 500 t yr^{-1} for the Arvorezinha catchment. As arable land (including fallow) covers 50–60% of the total catchment area (Fig. 1a), this would result in an average soil loss of ca. 7.5 t ha^{-1} yr^{-1} or 0.5–0.6 mm yr^{-1}, assuming a bulk density of 1300 kg m^{-3}. This would imply a loss of ca. 25 to ca. 60 mm of soil thickness over 50 to 100 years. Given the important local variations in soil thickness, such a reduction would be very difficult to detect, also because ^{137}Cs-derived erosion and deposition patterns show that erosion and deposition are not systematically related to topography (Minella et al., 2014, 2012).

The fact that soil thickness on the mid-slope sections has not been significantly reduced on the steepest slope section after 50–100 years of agricultural land use suggests that, at the landscape scale, water erosion may not have degraded the soil resource in the area as much as some local observations would suggest. This does not imply that human activity did not have any effect on soil thickness in the study area: tillage erosion may have resulted in a significant reduction in soil thickness on convexities and downslope of field borders. Soil truncation due to agricultural erosion has been documented at the landscape scale for temperate regions in e.g. Belgium (Rommens et al., 2005), Germany (Clemens and Stahr, 1994) and France (Chartin et al., 2013), which are characterized by moderate erosion rates that have been maintained over millennia. For the Belgian loess belt it was shown that landscape-scale patterns of erosion and deposition, as well as erosion and deposition rates, were indeed consistent with our understanding of the processes causing such truncation (Peeters et al., 2008; Van Oost et al., 2005). If water and tillage erosion rates would be maintained for a longer time period in our study area, soils would become (strongly) truncated as well.

4.4.2. Chemical weathering degree

Similar to soil thickness, LUCC had little effect on the soil weathering degree (Fig. 3, Table 4). It would, however, be too simplistic to assume from these observations that LUCC and agricultural practices have not affected weathering processes in general. LUCC leads to changes in hydrological pathways resulting in clear changes in weathering product fluxes (Robinet et al., 2018a) and also affects deep weathering because the reduction of evapotranspiration due to deforestation implies that more water will reach deep groundwater layers (Ameijeiras-Mariño et al., 2018). However, the effects of changes in weathering rates on the weathering degree of the soil material will only become apparent over much longer timescales. Similar to what was found in other areas, Brosens et al. (2020) showed that the weathering degree of soils in our study area evolves over timescales of > 10 000 years and that very often > 200 000 years is necessary for weathering processes to reach equilibrium with soil production and erosion. Therefore, changes in weathering *rates* over the last century will not have a measurable impact on observed weathering *degrees*.

Changes in weathering degree at the mid-slope section might still be observed due to the fact that LUCC dramatically accelerates physical erosion. We already discussed above that water erosion rates are likely to be too small to cause a significant change over the timescale of a century: if only a few cm of soil is lost, no measurable change in weathering degree in the remaining soil, generally being > 0.5 m thick is to be expected. Tillage erosion can be far more intense and may rapidly translocate deeply weathered topsoil from upslope positions to the mid-slope section. Van Oost et al. (2000) showed that such translocation can take place over distances exceeding 50 m in a century. However, we did not observe a significantly higher topsoil weathering degree on agricultural land (Fig. A.5). This is mainly explained by the fact that field parcels in the study area are generally small. This prevents topsoil material to be moved by tillage from the plateau area to the steep mid-slope section due to the presence of intermediate field boundaries.

The TRB, in general, sometimes behaves differently in comparison to other weathering indices which are based on the relative enrichment of immobile elements like the CIA, as the weathering of basaltic rock in a tropical climate can lead to a rapid loss of cations to secondary minerals (Caner et al., 2014; Chorover et al., 2004). However, in our study area, the CIA, TRB and Fe_d/Fe_t related well to each other (Table 2). This indicates that the leaching of released cations after weathering is fast enough to avoid a relative enrichment in the soils: this is not surprising given the high annual precipitation in the area (ca. 1900 mm, Robinet et al., 2018b, 2018a). On agricultural land, the external input of cations with fertilizers also influences an index like the TRB. Soil pore water sampled at shallow depth at the sites of the calibration/validation dataset indeed showed higher concentrations of base cations under cropland relative to sites under forest (Ameijeiras-Mariño et al., 2018). These higher concentrations were partially associated to the input of fertilizers. However, we did not find a statistically significant effect of land use on TRB, suggesting that the mobile cations present in fertilizer are quickly leached from the soil and/or that the amount of fertilizer applied is negligible with respect to non-exchangeable stocks (see Vanacker et al., 2019 for a more detailed discussion on this topic). Dust deposition can also influence an index like the TRB. This influence is likely limited as dust deposition is low in our study area (Zheng et al., 2016).

5. Conclusions

The overall objective of our study was to evaluate how deforestation and agricultural practices affected soil thickness and soil weathering degree in a subtropical region in Southern Brazil. We first showed that mid-infrared spectroscopy can be used to successfully estimate different weathering indices, thereby confirming that this technique can indeed be used to rapidly obtain information about soil weathering degree at a relatively large spatial scale. Our data highlighted slope gradient as the main explaining factor influencing the spatial variability of both the soil thickness and the soil chemical weathering degree in our study area. Other factors (soil thickness, sampling depth, elevation) also showed a strong association with weathering and soil thickness, but were strongly related with the slope gradient itself. On mid-slope sections soil thickness decreases with slope gradient due to the fact that water erosion intensity and diffusive soil transport are slope-dependent. The weathering degree is dependent on the soil residence time, which is controlled by slope steepness through the erosion - slope gradient and soil flux - slope gradient couplings. Neither soil thickness nor weathering degree showed important differences between forest and agricultural sites. This suggests that, while erosion rates can locally be very high after LUCC, this does not necessarily lead to a marked decrease in average soil thickness and/or fundamental changes in soil chemical properties after one century. Even on steep slopes this is the case, which are generally considered to be most sensitive to agricultural erosion. Assessments at the landscape scale may help to better assess how soils respond to LUCC and may complement point-scale studies that remain crucial to understand the impact of changes on the processes controlling the soil system.

Declaration of Competing Interest

The authors declare that they have no known competing financial interests or personal relationships that could have appeared to influence the work reported in this paper.

Acknowledgments

We would like to thank A. Schlessner and colleagues from the Department of Soils of the University of Santa Maria (RS, Brazil) for their help during the preparation of the field campaign and for all logistic issues. We also thank L. Fondu and E. Vassilieva from the Department of Earth and Environmental Sciences of the KU Leuven (Belgium) for their help in the measurement of the MIR reflectance of the soil samples and the analysis of the rock samples, and A. Iserentant and C. Givron from the analytical platform MOCA at UCLouvain for the soil chemical analyses. YAM and JR were supported by the Belgian Science Policy Office (BELSPO) in the framework of the Inter University Attraction Pole project (P7/24)): SOGLO – The soil system under global change. LB has been supported by the Belgian Development Cooperation through VLIR-UOS and received a doctoral grant from the Research Foundation Flanders (FWO, 11B6919N). SO is supported by the National Funds for Scientific Research FNRS (FC69480). We would like to thank the anonymous reviewers for their constructive and extensive feedback, enabling significant improvement of the manuscript.

Appendix A. Supplementary material

Supplementary data to this article can be found online at https://doi.org/10.1016/j.catena.2021.105698.

References

Akaike, H., 1987. Factor analysis and AIC. Psychometrika 52 (3), 317–332. https://doi.org/10.1007/BF02294359.

Alegre, J.C., Cassel, D.K., Bandy, D.E., 1986. Effects of Land Clearing and Subsequent Management on Soil Physical Properties. Soil Sci. Soc. Am. J. 50 (6), 1379–1384. https://doi.org/10.2136/sssaj1986.03615995005000060002x.

Alvares, C.A., Stape, J.L., Sentelhas, P.C., de Moraes Gonçalves, J.L., Sparovek, G., 2014. Köppen's climate classification map for Brazil. Meteorol. Zeitschrift 22 (6), 711–728. https://doi.org/10.1127/0941-2948/2013/0507.

Ameijeiras-Mariño, Y., Opfergelt, S., Derry, L.A., Robinet, J., Govers, G., Minella, J.P.G., Delmelle, P., 2018. Ge/Si ratios point to increased contribution from deeper mineral weathering to streams after forest conversion to cropland. Appl. Geochemistry 96, 24–34. https://doi.org/10.1016/j.apgeochem.2018.06.002.

Auerswald, K., Fiener, P., Dikau, R., 2009. Rates of sheet and rill erosion in Germany — A meta-analysis. Geomorphology 111 (3-4), 182–193. https://doi.org/10.1016/j.geomorph.2009.04.018.

Bakker, M.M., Govers, G., Rounsevell, M.D.A., 2004. The crop productivity–erosion relationship: an analysis based on experimental work. Catena 57 (1), 55–76. https://doi.org/10.1016/j.catena.2003.07.002.

Baptista, G.M.M., Corrêa, R.S., dos Santos, P.F., Madeira Netto, J.S., Meneses, P.R., 2011. Use of Imaging Spectroscopy for Mapping and Quantifying the Weathering Degree of Tropical Soils in Central Brazil. Appl. Environ. Soil Sci. 2011, 1–7. https://doi.org/10.1155/2011/641328.

Barnes, R.J., Dhanoa, M.S., Lister, S.J., 1989. Standard Normal Variate Transformation and De-Trending of Near-Infrared Diffuse Reflectance Spectra. Appl. Spectrosc. 43 (5), 772–777. https://doi.org/10.1366/0003702894202201.

Baumann, F., Schmidt, K., Dörfer, C., He, J.S., Scholten, T., Kühn, P., 2014. Pedogenesis, permafrost, substrate and topography: Plot and landscape scale interrelations of weathering processes on the central-eastern Tibetan Plateau. Geoderma 226–227, 300–316. https://doi.org/10.1016/j.geoderma.2014.02.019.

Baumler, R., 2004. Pedogenic studies in eastern Nepal - New aspects about the last glaciation. Quat. Sci. Rev. 23 (16-17), 1777–1783. https://doi.org/10.1016/j.quascirev.2004.03.003.

Bayer, A., Bachmann, M., Müller, A., Kaufmann, H., 2012. A Comparison of Feature-Based MLR and PLS Regression Techniques for the Prediction of Three Soil Constituents in a Degraded South African Ecosystem. Appl. Environ. Soil Sci. 2012, 1–20. https://doi.org/10.1155/2012/971252.

Bellieni, G., Comin-Chiaramonti, P., Marques, L.S., Melfi, A.J., Nardy, A.J.R., Papatrechas, C., Piccirillo, E.M., Roisenberg, A., Stolfa, D., 1986. Petrogenetic Aspects of Acid and Basaltic Lavas from the Paran Plateau (Brazil): Geological, Mineralogical and Petrochemical Relationships. J. Petrol. 27, 915–944. https://doi.org/10.1093/petrology/27.4.915.

Bertrand, I., Janik, L.J., Holloway, R.E., Armstrong, R.D., McLaughlin, M.J., 2002. The rapid assessment of concentrations and solid phase associations of macro- and micronutrients in alkaline soils by mid-infrared diffuse reflectance spectroscopy. Aust. J. Soil Res. 40, 1339–1356. https://doi.org/10.1071/SR01104.

Bortoluzzi, E.C., Moterle, D.F., dos Santos Rheinheimer, D., Casali, C.A., Melo, G.W., Brunetto, G., 2012. Mineralogical changes caused by grape production in a regosol from subtropical Brazilian climate. J. Soils Sediments 12 (6), 854–862. https://doi.org/10.1007/s11368-012-0509-x.

Brantley, S.L., Goldhaber, M.B., Ragnarsdottir, K.V., 2007. Crossing Disciplines and Scales to Understand the Critical Zone. Elements 3 (5), 307–314. https://doi.org/10.2113/gselements.3.5.307.

Brosens, L., Campforts, B., Robinet, J., Vanacker, V., Opfergelt, S., Ameijeiras-Mariño, Y., Minella, J.P.G., Govers, G., 2020. Slope Gradient Controls Soil Thickness and Chemical Weathering in Subtropical Brazil: Understanding Rates and Timescales of Regional Soilscape Evolution Through a Combination of Field Data and Modeling. J. Geophys. Res. Earth Surf. 125 https://doi.org/10.1029/2019JF005321 e2019JF005321.

Buettner, S.W., Kramer, M.G., Chadwick, O.A., Thompson, A., 2014. Mobilization of colloidal carbon during iron reduction in basaltic soils. Geoderma 221–222, 139–145. https://doi.org/10.1016/j.geoderma.2014.01.012.

Burke, B.C., Heimsath, A.M., White, A.F., 2007. Coupling chemical weathering with soil production across soil-mantled landscapes. Earth Surf. Process. Landforms 32 (6), 853–873. https://doi.org/10.1002/(ISSN)1096-9837.

Calderón, F.J., Reeves, J.B., Collins, H.P., Paul, E.a., 2011. Chemical Differences in Soil Organic Matter Fractions Determined by Diffuse-Reflectance Mid-Infrared Spectroscopy. Soil Sci. Soc. Am. J. 75, 568–579. https://doi.org/10.2136/sssaj2009.0375.

Caner, L., Radtke, L.M., Vignol-Lelarge, M.L., Inda, A.V., Bortoluzzi, E.C., Mexias, A.S., 2014. Basalt and rhyo-dacite weathering and soil clay formation under subtropical climate in southern Brazil. Geoderma 235–236, 100–112. https://doi.org/10.1016/j.geoderma.2014.06.024.

Cerdan, O., Poesen, J., Govers, G., Saby, N., Le Bissonnais, Y., Gobin, A., Vacca, A., Quinton, J., Auerswald, K., Klik, A., Kwaad, F.F.P.M., Roxo, M.J., 2006. Sheet and Rill Erosion, in: Sons, J. wiley & (Ed.), Soil Erosion in Europe. John Wiley & Sons, Ltd, Chichester, UK, pp. 501–513. Doi: 10.1002/0470859202.ch38.

Chartin, Caroline, Evrard, Olivier, Salvador-Blanes, Sébastien, Hinschberger, Florent, Van Oost, Kristof, Lefèvre, Irène, Daroussin, Joël, Macaire, J.-J., 2013. Quantifying and modelling the impact of land consolidation and field borders on soil redistribution in agricultural landscapes (1954–2009). Catena 110, 184–195. https://doi.org/10.1016/j.catena.2013.06.006.

Chorover, Jon, Amistadi, M.K., Chadwick, O.A., 2004. Surface charge evolution of mineral-organic complexes during pedogenesis in Hawaiian basalt. Geochim. Cosmochim. Acta 68 (23), 4859–4876. https://doi.org/10.1016/j.gca.2004.06.005.

Clemens, G., Stahr, K., 1994. Present and past soil erosion rates in catchments of the Kraichgau area (SW-Germany). Catena 22 (2), 153–168. https://doi.org/10.1016/0341-8162(94)90023-X.

Cobo, Juan Guillermo, Dercon, Gerd, Yekeye, Tsitsi, Chapungu, Lazarus, Kadzere, Chengetai, Murwira, Amon, Delve, Robert, Cadisch, Georg, 2010. Integration of mid-infrared spectroscopy and geostatistics in the assessment of soil spatial variability at landscape level. Geoderma 158 (3-4), 398–411. https://doi.org/10.1016/j.geoderma.2010.06.013.

Cornu, S., Montagne, D., Maguin, F., Lay, C.L., Chevallier, P., Cousin, I., 2007. Influence of human impacts on Albeluvisol analysed by X-ray microfluorescence: Relative evolution of the transforming front at the tongue scale. Sci. Total Environ. 377 (2-3), 244–254. https://doi.org/10.1016/j.scitotenv.2007.01.083.

Damé, R. de C.F., Teixeira-Gandra, C.F.A., Guedes, H.A.S., Silva, G.M. da, Silveira, S.C.R. da, 2016. Intensity-Duration-Frequency relationships: stochastic modeling and disaggregation of daily rainfall in the lagoa Mirim watershed, Rio Grande do Sul, Brazil. Eng. Agrícola 36, 492–502. Doi: 10.1590/1809-4430-Eng.Agric.v36n3p492-502/2016.

de Moraes, Jorge M., Schuler, Azeneth E., Dunne, Thomas, Figueiredo, Ricardo de O., Victoria, Reynaldo L., 2006. Water storage and runoff processes in plinthic soils under forest and pasture in eastern Amazonia. Hydrol. Process. 20 (12), 2509–2526. https://doi.org/10.1002/(ISSN)1099-108510.1002/hyp.v20:1210.1002/hyp.6213.

Delvaux, Bruno, Herbillon, Adrien J., Vielvoye, Léon, 1989. Characterization of a weathering sequence of soils derived from volcanic ash in Cameroon. Taxonomic, mineralogical and agronomic implications. Geoderma 45 (3-4), 375–388. https://doi.org/10.1016/0016-7061(89)90017-7.

Dixon, J.L., Heimsath, A.M., Kaste, J., Amundson, R., 2009. Climate-driven processes of hillslope weathering. Geology 37, 975–978. Doi: 10.1130/G30045A.1.

Don, A., Schumacher, J., Freibauer, A., 2011. Impact of tropical land-use change on soil organic carbon stocks - a meta-analysis. Glob. Chang. Biol. 17, 1658–1670. https://doi.org/10.1111/j.1365-2486.2010.02336.x.

Dwan, K., Gamble, C., Williamson, P.R., Kirkham, J.J., 2013. Systematic Review of the Empirical Evidence of Study Publication Bias and Outcome Reporting Bias — An Updated Review. PLoS One 8, e66844. Doi: 10.1371/journal.pone.0066844.

Ernesto, M., Pacca, I.G., Hiodo, F.Y., Nardy, A.J.R., 1990. Palaeomagnetism of the Mesozoic Serra Geral Formation, southern Brazil. Phys. Earth Planet. Inter. 64 (2-4), 153–175. https://doi.org/10.1016/0031-9201(90)90035-V.

Farr, Tom G., Rosen, Paul A., Caro, Edward, Crippen, Robert, Duren, Riley, Hensley, Scott, Kobrick, Michael, Paller, Mimi, Rodriguez, Ernesto, Roth, Ladislav, Seal, David, Shaffer, Scott, Shimada, Joanne, Umland, Jeffrey, Werner, Marian, Oskin, Michael, Burbank, Douglas, Alsdorf, Douglas, 2007. The Shuttle Radar Topography Mission. Rev. Geophys. 45 (2) https://doi.org/10.1029/2005RG000183.

Fiener, P., Wilken, F., Auerswald, K., 2019. Filling the gap between plot and landscape scale - Eight years of soil erosion monitoring in 14 adjacent watersheds under soil conservation at Scheyern, Southern Germany. Adv. Geosci. 48, 31–48. https://doi.org/10.5194/adgeo-48-31-2019.

Foley, J.A., 2011. Can We Feed the World & Sustain the Planet? Sci. Am. 305, 60–65. https://doi.org/10.1038/scientificamerican1111-60.

Forouzangohar, M., Baldock, J.A., Smernik, R.J., Hawke, B., Bennett, L.T., 2015. Mid-infrared spectra predict nuclear magnetic resonance spectra of soil carbon. Geoderma 247–248, 65–72. https://doi.org/10.1016/j.geoderma.2015.02.006.

Franco, A., Malhotra, N., Simonovits, G., 2014. Publication bias in the social sciences: Unlocking the file drawer. Science 345 (6203), 1502–1505. https://doi.org/10.1126/science:1255484.

Garzanti, Eduardo, Andó, Sergio, France-Lanord, Christian, Censi, Paolo, Vignola, Pietro, Galy, Valier, Lupker, Maarten, 2011. Mineralogical and chemical variability of fluvial sediments 2. Suspended-load silt (Ganga–Brahmaputra, Bangladesh). Earth Planet. Sci. Lett. 302 (1-2), 107–120. https://doi.org/10.1016/j.epsl.2010.11.043.

Geladi, P., MacDougall, D., Martens, H., 1985. Correction for Near-Infrared Reflectance Spectra of Meat. Appl. Spectrosc. 39, 491–500. https://doi.org/10.1366/0003702854248656.

Godfray, H.C. J., Beddington, J.R., Crute, I.R., Haddad, L., Lawrence, D., Muir, J.F., Pretty, J., Robinson, S., Thomas, S.M., Toulmin, C., 2010. Food Security: The Challenge of Feeding 9 Billion People. Science 327 (5967), 812–818. https://doi.org/10.1126/science:1185383.

Goulding, K.W.T., de Varennes, Amarilis, 2016. Soil acidification and the importance of liming agricultural soils with particular reference to the United Kingdom. Soil Use Manag. 32 (3), 390–399. https://doi.org/10.1111/sum.2016.32.issue-310.1111/sum.12270.

Govers, G., Quine, T.A., Desmet, P.J.J., Walling, D.E., 1996. The relative contribution of soil tillage and overland flow erosion to soil redistribution on agricultural land. Earth Surf. Process. Landforms 21, 929–946. https://doi.org/10.1002/(SICI)1096-9837(199610)21:10<929::AID-ESP631>3.0.CO;2-C.

Govers, G., Vandaele, K., Desmet, P., Poesen, J., Bunte, K., 1994. The role of tillage in soil redistribution on hillslopes. Eur. J. Soil Sci. 45 (4), 469–478. https://doi.org/10.1111/ejs.1994.45.issue-410.1111/j.1365-2389.1994.tb00532.x.

Guo, L.B., Gifford, R.M., 2002. Soil carbon stocks and land use change: a meta analysis. Glob. Chang. Biol. 8, 345–360. https://doi.org/10.1046/j.1354-1013.2002.00486.x.

Haghighi, F., Gorji, M., Shorafa, M., 2010. A study of the effects of land use changes on soil physical properties and organic matter. L. Degrad. Dev. 21 (5), 496–502. https://doi.org/10.1002/ldr.v21:510.1002/ldr.999.

Herbillon, A.J., 1986. Chemical estimation of weatherable minerals present in the diagnostic horizons of low activity clay soils, Proceedings of the 8th international Soil Classification Workshop: Classification, Characterization and Utilization of Oxisols Part 1. EMBRAPA, Rio de Janeiro.

Houben, Peter, 2008. Scale linkage and contingency effects of field-scale and hillslope-scale controls of long-term soil erosion: Anthropogeomorphic sediment flux in agricultural loess watersheds of Southern Germany. Geomorphology 101 (1-2), 172–191. https://doi.org/10.1016/j.geomorph.2008.06.007.

IBGE, (Instituto Brasileiro de Geografia e Estatística), 2003. Solos. Passo Fundo. SH. 22-V-B.

IUSS Working Group WRB, 2015. World Reference Base for Soil Resources 2014, update 2015 International soil classification system for naming soils and creating legends for soil maps. In: World Soil Resources Reports No, 106. FAO, Rome.

Lortie, C.J., Aarssen, L.W., Budden, A.E., Koricheva, J.K., Leimu, R., Tregenza, T., 2007. Publication bias and merit in ecology. Oikos 116 (7), 1247–1253. https://doi.org/10.1111/oik.2007.116.issue-710.1111/j.2007.0030-1299.15686.x.

Jahn, R., Blume, H., Asio, V.B., Spaargaren, O., Schad, P., 2006. Guidelines for soil description. Food Agric. Organ, Rome.

Janik, L., Skjemstad, J., Raven, M., 1995. Characterization and analysis of soils using mid-infrared partial least-squares.1. Correlations with XRF-determined major-element composition. Soil Res. 33, 621–636. https://doi.org/10.1071/SR9950621.

Janik, L.J., Merry, R.H., Skjemstad, J.O., 1998. Can mid infrared diffuse reflectance analysis replace soil extractions? Aust. J. Exp. Agric. 38, 681–696. https://doi.org/10.1071/EA97144.

Kicinski, M., 2014. How does under-reporting of negative and inconclusive results affect the false-positive rate in meta-analysis? A simulation study. BMJ Open 4 (8). https://doi.org/10.1136/bmjopen-2014-004831.

Labrière, N., Locatelli, B., Laumonier, Y., Freycon, V., Bernoux, M., 2015. Soil erosion in the humid tropics: A systematic quantitative review. Agric. Ecosyst. Environ. 203, 127–139. https://doi.org/10.1016/j.agee.2015.01.027.

Lal, R., 2001. Soil degradation by erosion. L. Degrad. Dev. 12 (6), 519–539. https://doi.org/10.1002/(ISSN)1099-145X10.1002/ldr.v12:610.1002/ldr.472.

Lambin, E.F., Geist, H.J., Lepers, E., 2003. Dynamics of Land-Use and Land-Cover Change in Tropical Regions. Annu. Rev. Environ. Resour. 28, 205–241. https://doi.org/10.1146/annurev.energy.28.050302.105459.

Le Bas, M.J., Streckeisen, A.L., 1991. The IUGS systematics of igneous rocks. J. Geol. Soc. London. 148 (5), 825–833. https://doi.org/10.1144/gsjgs.148.5.0825.

Le Gall, Marion, Evrard, Olivier, Dapoigny, Arnaud, Tiecher, Tales, Zafar, Mohsin, Minella, J.P.G., Laceby, J.P., Ayrault, Sophie, 2017. Tracing Sediment Sources in a Subtropical Agricultural Catchment of Southern Brazil Cultivated With Conventional and Conservation Farming Practices. L. Degrad. Dev. 28 (4), 1426–1436. https://doi.org/10.1002/ldr.v28.410.1002/ldr.2662.

Lemenih, Mulugeta, Karltun, Erik, Olsson, Mats, 2005. Assessing soil chemical and physical property responses to deforestation and subsequent cultivation in smallholders farming system in Ethiopia. Agric. Ecosyst. Environ. 105 (1-2), 373–386. https://doi.org/10.1016/j.agee.2004.01.046.

Lepers, E., Lambin, E.F., Janetos, A.C., DeFries, R., Achard, F., Ramankutty, N., Scholes, R.J., 2005. A Synthesis of Information on Rapid Land-cover Change for the Period 1981–2000. Bioscience 55, 115–124. https://doi.org/10.1641/0006-3568(2005)055[0115:ASOIOR]2.0.CO;2.

Lopes, F., 2006. Utilização do Modelo Century para avaliar a dinâmica do Carbono do solo em uma pequena bacia hidrográfica rural. Universidade Federal do Rio Grande Do Sul. http://hdl.handle.net/10183/7960.

Lucas, Y., 2001. The Role of Plants in Controlling Rates and Products of Weathering: Importance of Biological Pumping. Annu. Rev. Earth Planet. Sci. 29 (1), 135–163. https://doi.org/10.1146/annurev.earth.29.1.135.

Lundström, U.S., 1994. Significance of organic acids for weathering and the podzolization process. Environ. Int. 20 (1), 21–30. https://doi.org/10.1016/0160-4120(94)90063-9.

Madari, Beáta E., Reeves, James B., Machado, Pedro L.O.A., Guimarães, Cleber M., Torres, Eleno, McCarty, Gregory W., 2006. Mid- and near-infrared spectroscopic assessment of soil compositional parameters and structural indices in two Ferralsols. Geoderma 136 (1-2), 245–259. https://doi.org/10.1016/j.geoderma.2006.03.026.

McDowell, William H., Asbury, Clyde E., 1994. Export of carbon, nitrogen, and major ions from three tropical montane watersheds. Limnol. Oceanogr. 39 (1), 111–125. https://doi.org/10.4319/lo.1994.39.1.0111.

Mehra, O.P., Jackson, M.L., 1958. Iron Oxide Removal from Soils and Clays by a Dithionite-Citrate System Buffered with Sodium Bicarbonate. Clays Clay Miner. 7, 317–327. https://doi.org/10.1346/CCMN.1958.0070122.

Minasny, Budiman, Tranter, Grant, McBratney, Alex. B., Brough, Daniel M., Murphy, Brian W., 2009. Regional transferability of mid-infrared diffuse reflectance spectroscopic prediction for soil chemical properties. Geoderma 153 (1-2), 155–162. https://doi.org/10.1016/j.geoderma.2009.07.021.

Minella, J.P.G., Merten, G.H., Walling, D.E., Moro, M., 2012. Using Cs-137 measurements and sediment yield monitoring to document catchment-scale sediment dynamics and budgets. Eros. Sediment Yields Chang. Environ. 356, 338–344. https://iahs.info/uploads/dms/15828.51-338-344-356-14-ICCE2012_Jean-P.G.-Minella-44-.pdf.

Minella, J.P.G., Merten, G.H., Walling, D.E., Reichert, J.M., 2009. Changing sediment yield as an indicator of improved soil management practices in southern Brazil. Catena 79 (3), 228–236. https://doi.org/10.1016/j.catena.2009.02.020.

Minella, J.P.G., Walling, D.E., Merten, G.H., 2014. Establishing a sediment budget for a small agricultural catchment in southern Brazil, to support the development of effective sediment management strategies. J. Hydrol. 519, 2189–2201. https://doi.org/10.1016/j.jhydrol.2014.10.013.

Mohanty, B., Gupta, A., Das, B.S., 2016. Estimation of weathering indices using spectral reflectance over visible to mid-infrared region. Geoderma 266, 111–119. https://doi.org/10.1016/j.geoderma.2015.11.030.

Morellato, L.P.C., Haddad, C.F.B., 2000. Introduction : The Brazilian Atlantic Forest. Boitropica 32, 786–792. https://www.jstor.org/stable/2663917.

Nesbitt, H.W., Young, G.M., 1982. Early Proterozoic climates and plate motions inferred from major element chemistry of lutites. Nature 299 (5885), 715–717. https://doi.org/10.1038/299715a0.

Nocita, M., Stevens, A., van Wesemael, B., Aitkenhead, M., Bachmann, M., Barthès, B., Ben Dor, E., Brown, D.J., Clairotte, M., Csorba, A., Dardenne, P., Demattê, J.A.M., Genot, V., Guerrero, C., Knadel, M., Montanarella, L., Noon, C., Ramirez-Lopez, L., Robertson, J., Sakai, H., Soriano-Disla, J.M., Shepherd, K.D., Stenberg, B., Towett, E. K., Vargas, R., Wetterlind, J., 2015. Soil Spectroscopy: An Alternative to Wet Chemistry for Soil Monitoring, in: Advances in Agronomy. pp. 139–159. Doi: 10.1016/bs.agron.2015.02.002.

Panagos, P., Borrelli, P., Meusburger, K., Yu, B., Klik, A., Jae Lim, K., Yang, J.E., Ni, J., Miao, C., Chattopadhyay, N., Sadeghi, S.H., Hazbavi, Z., Zabihi, M., Larionov, G.A., Krasnov, S.F., Gorobets, A.V., Levi, Y., Erpul, G., Birkel, C., Hoyos, N., Naipal, V., Oliveira, P.T.S., Bonilla, C.A., Meddi, M., Nel, W., Al Dashti, H., Boni, M., Diodato, N., Van Oost, K., Nearing, M., Ballabio, C., 2017. Global rainfall erosivity assessment based on high-temporal resolution rainfall records. Sci. Rep. 7, 4175. https://doi.org/10.1038/s41598-017-04282-8.

Peeters, Iris, Van Oost, Kristof, Govers, Gerard, Verstraeten, Gert, Rommens, Tom, Poesen, Jean, 2008. The compatibility of erosion data at different temporal scales. Earth Planet. Sci. Lett. 265 (1-2), 138–152. https://doi.org/10.1016/j.epsl.2007.09.040.

Pirie, A., Singh, B., Islam, K., 2005. Ultra-violet, visible, near-infrared, and mid-infrared diffuse reflectance spectroscopic techniques to predict several soil properties. Soil Res. 43, 713–721. https://doi.org/10.1071/SR04182.

Price, J.R., Velbel, M.A., 2003. Chemical weathering indices applied to weathering profiles developed on heterogeneous felsic metamorphic parent rocks. Chem. Geol. 202 (3-4), 397–416. https://doi.org/10.1016/j.chemgeo.2002.11.001.

Rasmussen, C., Brantley, S., Richter, D.B., Blum, A., Dixon, J., White, A.F., 2011. Strong climate and tectonic control on plagioclase weathering in granitic terrain. Earth Planet. Sci. Lett. 301 (3-4), 521–530. https://doi.org/10.1016/j.epsl.2010.11.037.

Reeves, J.B., Smith, D.B., 2009. The potential of mid- and near-infrared diffuse reflectance spectroscopy for determining major- and trace-element concentrations in soils from a geochemical survey of North America. Appl. Geochem. 24 (8), 1472–1481. https://doi.org/10.1016/j.apgeochem.2009.04.017.

Renne, P.R., Ernesto, M., Pacca, I.G., Coe, R.S., Glen, J., Prevot, M., Perrin, M., 1992. The age of Parana flood vulcanism, rifting of Gondwanaland, and the Jurassic-Crectaceous boundary. Science 258, 975–979. https://doi.org/10.1126/science.258.5084.975.

Ribeiro, M.C., Metzger, J.P., Martensen, A.C., Ponzoni, F.J., Hirota, M.M., 2009. The Brazilian Atlantic Forest: How much is left, and how is the remaining forest distributed? Implications for conservation. Biol. Conserv. 142 (6), 1141–1153. https://doi.org/10.1016/j.biocon.2009.02.021.

Richter, N., Jarmer, T., Chabrillat, S., Oyonarte, C., Hostert, P., Kaufmann, H., 2009. Free Iron Oxide Determination in Mediterranean Soils using Diffuse Reflectance Spectroscopy. Soil Sci. Soc. Am. J. 73 (1), 72–81. https://doi.org/10.2136/sssaj2008.0025.

Rinnan, Åsmund, Berg, Frans van den, Engelsen, Søren Balling, 2009. Review of the most common pre-processing techniques for near-infrared spectra. TrAC Trends Anal. Chem. 28 (10), 1201–1222. https://doi.org/10.1016/j.trac.2009.07.007.

Robinet, J., Minella, J.P. G., de Barros, C.A. P., Schlesner, Alexandre, Lücke, Andreas, Ameijeiras-Mariño, Yolanda, Opfergelt, Sophie, Vanderborght, Jan, Govers, Gerard, 2018a. Impacts of forest conversion and agriculture practices on water pathways in Southern Brazil. Hydrol. Process. 32 (15), 2304–2317. https://doi.org/10.1002/hyp.v32.1510.1002/hyp.13155.

Robinet, J., von Hebel, C., Govers, G., van der Kruk, J., Minella, J.P.G., Schlesner, A., Ameijeiras-Mariño, Y., Vanderborght, J., 2018b. Spatial variability of soil water content and soil electrical conductivity across scales derived from Electromagnetic Induction and Time Domain Reflectometry. Geoderma 314, 160–174. https://doi.org/10.1016/j.geoderma.2017.10.045.

Rommens, Tom, Verstraeten, Gert, Lang, Andreas, Poesen, Jean, Govers, Gerard, Van Rompaey, Anton, Lang, Andreas, Peeters, Iris, 2005. Soil erosion and sediment deposition in the Belgian oess belt during the Holocene: establishing a sediment budget for a small agricultural catchment. Holocene 15 (7), 1032–1043. https://doi.org/10.1191/0959683605hl876ra.

Salemi, L.F., Groppo, J.D., Trevisan, R., de Moraes, J.M., de Barros Ferraz, S.F., Villani, J. P., Duarte-Neto, P.J., Martinelli, L.A., 2013. Land-use change in the Atlantic rainforest region: Consequences for the hydrology of small catchments. J. Hydrol. 499, 100–109. https://doi.org/10.1016/j.jhydrol.2013.06.049.

Savitzky, Abraham., Golay, M.J.E., 1964. Smoothing and Differentiation of Data by Simplified Least Squares Procedures. Anal. Chem. 36 (8), 1627–1639. https://doi.org/10.1021/ac60214a047.

Schoonejans, J., Vanacker, V., Opfergelt, S., Christl, M., 2017. Long-term soil erosion derived from in-situ 10Be and inventories of meteoric 10Be in deeply weathered soils in southern Brazil. Chem. Geol. 466, 380–388. https://doi.org/10.1016/j.chemgeo.2017.06.025.

Soriano-Disla, José M., Janik, Les J., Viscarra Rossel, Raphael A., Macdonald, Lynne M., McLaughlin, Michael J., 2014. The Performance of Visible, Near-, and Mid-Infrared Reflectance Spectroscopy for Prediction of Soil Physical, Chemical, and Biological Properties. Appl. Spectrosc. Rev. 49 (2), 139–186. https://doi.org/10.1080/05704928.2013.811081.

Stevens, A., Ramirez Lopez, L., 2014. An introduction to the prospectr package 1–22. Doi: http://cran.r-project.org/web/packages/prospectr/vignettes/prospectr-intro.pdf.

Trabaquini, Kleber, Formaggio, Antônio Roberto, Galvão, Lênio Soares, 2015. Changes in Physical Properties of Soils with Land Use Time in the Brazilian Savanna Environment. L. Degrad. Dev. 26 (4), 397–408. https://doi.org/10.1002/ldr.2222.

Turner, Simon, Regelous, Marcel, Kelley, Simon, Hawkesworth, Chris, Mantovani, Marta, 1994. Magmatism and continental break-up in the South Atlantic: high precision40Ar-39Ar geochronology. Earth Planet. Sci. Lett. 121 (3-4), 333–348. https://doi.org/10.1016/0012-821X(94)90076-0.

van Breemen, N., Mulder, J., Driscoll, C.T., 1983. Acidification and alkalinization of soils. Plant Soil 75 (3), 283–308. https://doi.org/10.1007/BF02369968.

Van Oost, K., Govers, G., De Alba, S., Quine, T.A., 2006. Tillage erosion: a review of controlling factors and implications for soil quality. Prog. Phys. Geogr. Earth Environ. 30 (4), 443–466. https://doi.org/10.1191/0309133306pp487ra.

Van Oost, K., Govers, G., Desmet, P., 2000. Evaluating the effects of changes in landscape structure on soil erosion by water and tillage. Landsc. Ecol. 15, 577–589. https://doi.org/10.1023/A:1008198215674.

Van Oost, K., Van Muysen, W., Govers, G., Deckers, J., Quine, T.A., 2005. From water to tillage erosion dominated landform evolution. Geomorphology 72 (1-4), 193–203. https://doi.org/10.1016/j.geomorph.2005.05.010.

Vanacker, V., Ameijeiras-Mariño, Y., Schoonejans, J., Cornélis, J., Minella, J.P.G., Lamouline, F., Vermeire, M., Campforts, B., Robinet, J., Van de Broek, M., Delmelle, P., Opfergelt, S., 2019. Land use impacts on soil erosion and rejuvenation in Southern Brazil. Catena 178, 256–266. https://doi.org/10.1016/j.catena.2019.03.024.

Veldkamp, E., 1994. Organic Carbon Turnover in Three Tropical Soils under Pasture after Deforestation. Soil Sci. Soc. Am. J. 58 (1), 175–180. https://doi.org/10.2136/sssaj1994.03615995005800010025x.

Vieira, B.C., Salgado, A.A.R., dos Santos, L.J.C., 2015. Landscapes and Landforms of Brazil, World Geomorphological Landscapes. Springer Netherlands, Dordrecht. Doi: 10.1007/978-94-017-8023-0.

White, Art F., Blum, Alex E., Schulz, Marjorie S., Vivit, Davison V., Stonestrom, David A., Larsen, Matthew, Murphy, Sheila F., Eberl, D., 1998. Chemical Weathering in a Tropical Watershed, Luquillo Mountains, Puerto Rico: I. Long-Term Versus Short-Term Weathering Fluxes. Geochim. Cosmochim. Acta 62 (2), 209–226. https://doi.org/10.1016/S0016-7037(97)00335-9.

Zeaiter, M., Roger, J.-M., Bellon-Maurel, V., 2005. Robustness of models developed by multivariate calibration. Part II: The influence of pre-processing methods. TrAC Trends Anal. Chem. 24 (5), 437–445. https://doi.org/10.1016/j.trac.2004.11.023.

Zhao, L., Hong, H., Liu, J., Fang, Q., Yao, Y., Tan, W., Yin, K., Wang, C., Chen, M., Algeo, T.J., 2018. Assessing the utility of visible-to-shortwave infrared reflectance spectroscopy for analysis of soil weathering intensity and paleoclimate reconstruction. Palaeogeogr. Palaeoclimatol. Palaeoecol. 512, 80–94. https://doi.org/10.1016/j.palaeo.2017.07.007.

Zheng, Y., Zhao, T., Che, H., Liu, Y., Han, Y., Liu, C., Xiong, J., Liu, J., Zhou, Y., 2016. A 20-year simulated climatology of global dust aerosol deposition. Sci. Total Environ. 557–558, 861–868. https://doi.org/10.1016/j.scitotenv.2016.03.086.